NCAT Report 12-05

EFFECT OF REJUVENATOR ON PERFORMANCE PROPERTIES OF HMA MIXTURES WITH HIGH RAP AND RAS CONTENTS

By

Nam H. Tran, Ph.D., P.E., LEED GA
Adam Taylor, P.E.
Richard Willis, Ph.D.

June 2012

National Center for Asphalt Technology
NCAT
at AUBURN UNIVERSITY

277 Technology Parkway ■ Auburn, AL 36830

EFFECT OF REJUVENATOR ON PERFORMANCE PROPERTIES OF HMA MIXTURES WITH HIGH RAP AND RAS CONTENTS

By

Nam Tran, Ph.D., P.E., LEED GA
Adam Taylor, P.E.
Richard Willis, Ph.D.

National Center for Asphalt Technology
Auburn University, Auburn, Alabama

Sponsored by

NAPA Research and Education Foundation

June 2012

ACKNOWLEDGEMENTS

This project was sponsored by the NAPA Research and Education Foundation. The project would like to thank the foundation for their sponsorship of this project and the members of NCAT Application Steering Committee for reviewing this report.

DISCLAIMER

The contents of this report reflect the views of the authors who are responsible for the facts and accuracy of the data presented herein. The contents do not necessarily reflect the official views or policies of the NAPA Research and Education Foundation or the National Center for Asphalt Technology, or Auburn University. This report does not constitute a standard, specification, or regulation. Comments contained in this report related to specific testing equipment and materials should not be considered an endorsement of any commercial product or service; no such endorsement is intended or implied.

TABLE OF CONTENTS

LIST OF TABLES

LIST OF FIGURES

1 INTRODUCTION

The cost of materials and energy has significantly increased for the last few years. As a result reclaimed asphalt pavements (RAP) and/or reclaimed asphalt shingles (RAS) have been increasingly used in asphalt mixtures to replace virgin asphalt and aggregate materials and to reduce mixture costs. Each year, it is estimated that about 100 million tons of asphalt pavement materials are milled off roads (*1*). In addition, approximately 11 million tons of asphalt shingles are disposed. Of this amount, 10 million tons are from installation scraps and tear-offs from re-roofing, and one million tons are from asphalt shingle manufacturers (*2*). The use of these recycled materials in hot-mix asphalt (HMA) reduces costs for manufacturers and consumers as well as the negative environmental impacts associated with the extraction, transportation, and processing of virgin materials. Using RAS, especially shingle tear-offs, in HMA also conserves valuable landfill space.

Currently, most highway agencies allow asphalt mixtures containing low percentages of RAP (i.e., less than 25 percent by weight of aggregate) and/or up to five percent manufacturer's shingle scrap. The reason is that the recycled binder in the RAP and RAS is aged and stiffer than the binder in a virgin mixture selected for the same location. The primary barriers to recycling tear-offs are varying material composition and contaminants. The recycled binder is less strain-tolerant, and it may be more susceptible to various modes of cracking (i.e., fatigue, thermal, and reflection cracking). As the percentage of recycled binder increases, the proportion of the aged binder in the total binder blend increases, likely resulting in higher mixture stiffness and lower resistance to cracking. Transportation agencies are concerned that the use of asphalt mixtures with high recycled binder contents would significantly reduce the performance of asphalt pavements, causing higher pavement maintenance and rehabilitation costs. Therefore, before allowing the use of higher RAP/RAS contents in HMA, agencies want to ensure that these mixtures will provide satisfactory performance.

To offset the higher binder stiffness and improve the mixture resistance to cracking when high RAP/RAS contents are used, three approaches may be considered. The first approach is to use a softer virgin binder to blend with the recycled binder to achieve the desired performance grade (PG) of the binder blend through a blending chart (*3*). The second approach is to lower the design air voids (e.g., from 4% to 2%) to increase the total binder content in the asphalt mixture to improve the cracking resistance. This is the same approach that is used to design a rich bottom-layer mix. The third approach is to use a recycling agent (i.e., a rejuvenator) to restore the performance properties of recycled binder. A recent study conducted by Mallick et al. (*4*) showed promising results of asphalt mixtures using 100 percent RAP that had been rejuvenated with Reclamite®. The focus of the research presented in this report is on the third approach.

Rejuvenators have been used as recycling agents to restore some performance properties of oxidized RAP binders for cold in-place recycling and as surface treatment emulsions to preserve weathered asphalt pavements. However, they have not been widely used in HMA containing high recycled binder contents because of the uncertain effect of rejuvenators, the concern for the lack of adequate mixing of the old binder and the rejuvenator, and the required reaction time on performance properties of the recycled binders and asphalt mixtures. If an appropriate amount of rejuvenator is added and properly mixed, and required reaction time is allowed, the recycled

RAP binder may meet the target performance grade, resulting in improved cracking resistance of the asphalt mixture without adversely affecting its resistance to rutting.

1.1 Objective

The objective of this study is to evaluate the effect of using a rejuvenator pre-blended with a virgin asphalt binder on performance properties of recycled binders and HMA mixtures with high RAP and RAS contents and to conduct a cost comparison of HMA mixtures when RAP and/or RAS are used.

2 BACKGROUND

2.1 Aging of Asphalt Binder

The structure of petroleum asphalt is regarded as a colloid in which asphaltenes are the dispersed phase and maltenes are the dispersion medium. Most paving asphalt binders have micelles of asphaltenes diluted in a fairly well-structured dispersion medium. In the dispersion medium, the asphaltenes form aggregates but are unable to create a continuous network (*5*). Physical changes in asphalt binder over time are dependent on changes in its chemical composition. As asphalt binder ages, some of the maltene medium is transformed into the asphaltene phase, resulting in higher asphaltene and lower maltene contents. When there are fewer maltenes available to disperse the asphaltenes, the asphaltenes will flocculate. This leads to higher viscosity and lower ductility, which influences the ability of asphalt binder to stretch without breaking (*6*). In other words, when the asphaltene micelles are not sufficiently mobile to flow past one another under the applied stress, the resistance of asphalt binder to cracking or fracture is decreased (*7*).

The aging of asphalt binder occurs in two stages: short-term and long-term. Short-term aging is mainly due to volatilization and/or absorption of oily components in the maltenes during mixing and construction. Long-term aging happens in the field and is due to changes in composition through reaction between asphalt constituents and atmospheric oxygen, chemical reaction between molecular components (polymerization), and formation of a structure within the asphalt binder (thixotropy) (*8*).

2.2 Rejuvenation and Diffusion of Asphalt Binder

To restore its rheological properties, an aged asphalt binder may be mixed with a recycling agent, which can be a softening agent or a rejuvenator. While softening agents such as asphalt flux oil, lube stock, and slurry oil can lower the viscosity of the aged binder, rejuvenators help restore the physical and chemical properties (*8*). Rejuvenators often consist of lubricating oil extracts and extender oils, which contain a high proportion of maltene constituents—napthenic or polar aromatic fractions—that help re-balance the composition of the aged binder that lost its maltenes during construction and service (*9*). While rejuvenators should have a high proportion of aromatics, which are necessary to keep the asphaltenes dispersed, they should contain a low content of saturates, which are highly incompatible with the asphaltenes (*10*, *11*).

The effectiveness of a rejuvenator depends on the uniform dispersion of the rejuvenator within the recycled mixture and the diffusion of the rejuvenator into the aged binder coated outside of the aggregate. The dispersion of rejuvenators within recycled mixtures at different plants was investigated by Lee et al. (*12*). The researchers visually detected the dyes that had been mixed with the rejuvenators. The authors concluded that uniform distribution of the rejuvenators could be accomplished through mechanical mixing at the plants.

According to Carpenter and Wolosick (*13*), the diffusion of a rejuvenator into an aged binder consists of the following four steps.

1. The rejuvenator forms a very low viscosity layer surrounding the asphalt-coated aggregate.
2. The rejuvenator starts to penetrate into the aged binder layer, decreasing the amount of raw rejuvenator surrounding the aggregate and softening the aged binder.
3. When no raw rejuvenator remains, the penetration of the rejuvenator still continues, decreasing the viscosity of the inner layer and gradually increasing the viscosity of the outer layer.
4. After a certain time, equilibrium is approached over the majority of the recycled binder film.

The aforesaid concept of diffusion process was verified by Carpenter and Wolosick (*13*) through a staged extraction method in which the inner and outer layers of the rejuvenated binder film were extracted separately at predetermined time intervals. Figure 1 shows the penetration values at 25°C for each layer as a function of time after mixing, and the two layers approach the same consistency, which is close to that of a mixture of the same rejuvenator and recycled binder contents. The researchers concluded that the diffusion of the rejuvenator into the aged binder occurred during mixing, construction and a period of time in service life of pavement. These findings were later confirmed by Noureldin and Wood (*14*) and Huang et al. (*15*). According to Karlsson and Isacsson (*16*), the diffusion rate is governed by the viscosity of the maltene phase rather than the viscosity of the recycled binder as a whole. An earlier study by Oliver (*17*) suggested that the diffusion could be accelerated by adding diluent oil fractions and/or raising the mixing and compaction temperatures.

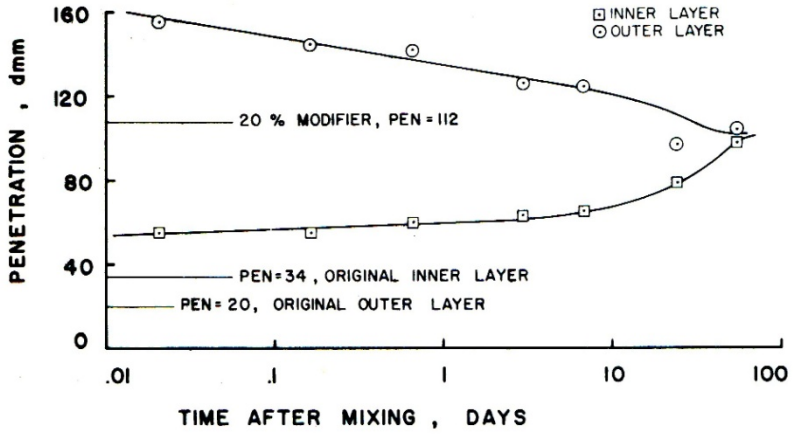

Figure 1 Penetration of the Outer and Inner Layers during Diffusion (*13*)

2.3 Performance of Rejuvenated Asphalt Binders and Mixtures

Rejuvenated RAP and/or RAS can be mixed with a virgin binder and aggregate to achieve a desired performance grade (PG) and design gradation for an asphalt mixture. The performance of the blended binder, which is affected by the diffusion and/or mixing of the recycled and virgin binders in the blend, significantly affects the performance of the resulting asphalt mixture. The diffusion and mixing of binders in a blend depends upon a number of factors, including compatibility of binders, temperature of mixing, performance grade of virgin and recycled binder, and the percentage of recycled binder in the blended binder (*18*).

Past studies reported that the diffusion process may not be completed after the construction (*13*, *19*); thus, higher rutting rates were initially observed on roadways and on test sections subjected to accelerated pavement testing (*20*). Rejuvenated asphalt mixtures also showed higher susceptibility to low-temperature cracking compared to virgin mixtures when they had not been sufficiently rejuvenated (*21*). According to Terrel and Fritchen (*22*) and DeKold and Amirkhanian (*23*), the moisture susceptibility of recycled mixtures was similar to or improved over that of virgin mixtures. However, if stripping-susceptible mixtures were recycled, the moisture susceptibility may increase, and anti-stripping additives should be used appropriately (*23*). The type of rejuvenator used had little effect on moisture susceptibility (*24*).

3 RESEARCH PLAN

This section describes a testing plan that was set up to evaluate the effect of a rejuvenator on the performance of HMA mixtures with high RAP and RAS contents. First, materials selected for this study are discussed, followed by plans for testing asphalt binders and mixtures.

3.1 Materials

Virgin aggregates and RAP used in this study were sampled from the East Alabama Paving (EAP), Inc. plant in Opelika, Alabama. The RAP material had been crushed to pass a ½-in. sieve at the EAP plant. The RAS material used in this project was from asphalt shingle manufacturing waste and provided by C. W. Matthews Contracting Co., Inc. in Atlanta, Georgia.

Three 9.5-mm mix designs, including a virgin (control) mix design, a 50% RAP mix design, and a 20% RAP plus 5% RAS mix design, were used in this study. The virgin binder used in the mix designs was a PG 67-22. For each mix, 0.5% liquid anti-strip AD-here® LOF 65 (by weight of the virgin asphalt binder) manufactured by ArrMaz Custom Chemicals was added to the virgin binder before mixing.

The rejuvenator selected for this study is Cyclogen® L, which does not contain asphalt binder. A sample of this rejuvenator was provided by Tricor Refining, LLC in California. While the diffusion of rejuvenator into the recycled binder would be better if the rejuvenator was mixed with RAP and/or RAS before the RAP/RAS materials were added into the mix, this process would be difficult to implement in the field. Hence, in this study, the rejuvenator was added to the virgin binder, and then the blend was added to the mix of virgin aggregate and RAP/RAS materials for two mix designs—50% RAP mix design and 20% RAP plus 5% RAS mix design.

A total of five mixtures, including a control mix, a 50% RAP mix, a 20% RAP plus 5% RAS mix, a 50% RAP mix with rejuvenator, and a 20% RAP plus 5% RAS mix with rejuvenator, were evaluated in this study.

3.2 Plan for Binder Testing

Testing of virgin and recycled asphalt binders was conducted in two steps. The first step was to determine: (1) the effect of the rejuvenator on the performance properties of the recycled binders extracted from RAP and RAS; and (2) the amount of rejuvenator required to restore the performance properties of the recycled binders to meet the requirements for a PG 67-22, which is the performance grade of the virgin binder used in the mix designs. The second step was to determine the properties of the blends of recycled binders, virgin binder and rejuvenator. The rejuvenator was mixed with the virgin binder at the optimum content determined in the first step. Then, the blend was mixed with the binders extracted from RAP and RAS based on the amount of each binder determined in the 50% RAP mix design and 20% RAP plus 5% RAS mix design. The purpose of this testing was to determine the true grade of each blend and to make sure that there were no compatibility issues. A detailed description of each step follows.

In the first step, the extracted RAP/RAS binder was heated to 135^{o}C and then thoroughly blended with the rejuvenator at the blending rates shown in Table 1. A total of six blends were tested in the first step. For each blend, a portion was tested in the dynamic shear rheometer (DSR) to determine the high temperature properties. The rest of the blend was long-term aged in the pressure-aging vessel (PAV). The PAV-aged binder was then tested in the DSR to determine the intermediate temperature properties and in the bending-beam rheometer (BBR) to determine the low-temperature properties. Results of this testing were used to determine (1) the effect of rejuvenator on the RAP and RAS binders and (2) the optimum amount of the rejuvenator required to restore the performance properties of the recycled binders to meet the requirements for a PG 67-22.

Table 1 Step 1 of Binder Testing

Summary of Experiment		
Attribute	**Level**	**Description**
Materials		
RAP Binder	1	Binder extracted from RAP
RAS Binder	1	Binder extracted from RAS
Rejuvenator (Cyclogen L)		
Blending Rate for RAP	3	0, 12, 20% by weight of RAP binder
Blending Rate for RAS	3	0, 10, 20% by weight of RAP binder
No. of Blends	6	1×3 (for RAP) + 1×3 (for RAS) = 6
Response Variable		True Grade

After the optimum amount of the rejuvenator required to restore the performance properties of the recycled binders was determined, the mix designs were conducted. Based on the amount of each binder in the five mixtures tested in this study, the virgin binder and four binder blends were prepared and evaluated in the second step, as shown in Table 2. For each blend, the performance grade was determined in accordance with AASHTO M 320. In addition, the linear

amplitude sweep (LAS) test was conducted based on a proposed test procedure developed at the Modified Asphalt Research Center at the University of Wisconsin-Madison to evaluate the cracking resistance of each binder blend. Results of this testing was used to determine the properties of the blends and to compare results with those of the virgin binder.

Table 2 Step 2 of Binder Testing

Summary of Experiment		
Attribute	**Level**	**Description**
Materials		
Control	1	Virgin binder (PG 67-22)
50% RAP	1	Virgin binder + extracted RAP binder
50% RAP with Rejuvenator	1	Virgin binder + extracted RAP binder + rejuvenator
20% RAP plus 5% RAS	1	Virgin binder + extracted RAP and RAS binders
20% RAP plus 5% RAS with Rejuvenator	1	Virgin binder + extracted RAP and RAS binders + rejuvenator
No. of Blends	5	1 + 1 + 1 + 1+ 1 = 5
Response Variables		Performance grade (PG) and LAS results

3.3 Plan for Mixture Testing

Due to the time-dependent diffusion process of the rejuvenators, asphalt mixtures were tested in both short- and long-term aged conditions. The short- and long-term properties were used to evaluate the mixture resistance to permanent deformation and cracking, respectively. The following paragraphs describe the process for preparing samples and laboratory tests conducted for short-term and long-term aged specimens.

To prepare an asphalt mixture for this study, the virgin binder, virgin aggregates and RAP were heated in an oven to the target mixing temperature of 300^{o}F, and the RAS were kept at the room temperature. The liquid anti-strip was pre-blended with the virgin binder. The rejuvenator was also pre-blended with the virgin binder at its optimum content determined in the first step of binder testing. The mixing process was done in several steps. The virgin aggregates were first poured into a mixing bowl. If used, the RAP and/or RAS were then added into the bowl and mixed with the virgin aggregates. After that, the virgin binder, which had been pre-blended with the liquid anti-strip and rejuvenator (if used), was thoroughly added to the mixture.

The mix was short-term aged in an oven according to AASHTO R 30 for determining the volumetric properties and for mechanical testing or according to AASHTO T 283 for the tensile strength ratio (TSR) test. The asphalt sample was then compacted, and the specimen was prepared for further testing.

The TSR test was conducted to determine the mix resistance to moisture damage. Two tests, including the dynamic modulus (E*) and the Asphalt Pavement Analyzer (APA), were conducted on the short-term aged specimens to determine the short-term aged stiffness and to evaluate the mix resistance to permanent deformation.

To determine the long-term properties, the test specimens cored/cut from the gyratory specimens were long-term aged in an oven at 85°C for 120 hours according to AASHTO R 30. Four tests were performed on the long-term aged specimens: E* to determine stiffness of the long-term aged mixture, indirect tensile (IDT) to determine the critical low-temperature cracking properties, and two tests (Energy Ratio (ER) and Overlay Tester (OT)) to determine the mix resistance to cracking at intermediate temperatures. Table 3 summarizes the plan for mixture testing.

Table 3 Plan for Mixture Testing

Summary of Experiment		
Attribute	**Level**	**Description**
Asphalt Mixtures		
Control	1	Virgin aggregates and binder
50% RAP	1	With 50% RAP but no rejuvenator
50% RAP with Rejuvenator	1	With 50% RAP and rejuvenator
20% RAP plus 5% RAS	1	With 20% RAP plus 5% RAS but no rejuvenator
20% RAP plus 5% RAS with Rejuvenator	1	With 20% RAP plus 5% RAS and rejuvenator
No. of Mixtures	5	1 + 1 + 1 + 1 + 1 = 5
Response Variable		Volumetric properties TSR Short-term aged: E* and APA Long-term aged: E*, IDT, ER and OT

4 RESULTS AND ANALYSIS

In this section, the determination of optimum rejuvenator content is first discussed, followed by the mix design properties, and finally results of binder and mixture tests.

4.1 Rejuvenator Content

As discussed in the plan for testing binder, the rejuvenator was blended at three contents with the binders extracted from the RAP and RAS. Then, the performance grades of the blends were determined in accordance with AASHTO M 320. Detailed results are presented in Appendix A.

Figure 2 and Figure 3 show the effect of the rejuvenator contents on the performance properties of the RAP and RAS binders. The correlations between the rejuvenator contents and the critical high and low temperatures of the RAP and RAS binders are almost linear, as the R^2 values are greater than 0.95. Based on the correlations, a content of 12% by the total weight of recycled binders was selected based on the critical low temperature criteria. At this content, the critical high temperature criteria were also satisfied, and the performance properties of the recycled binders would be restored to meet the requirements for a PG 67-22, which is the performance grade of the virgin binder used in the mix designs.

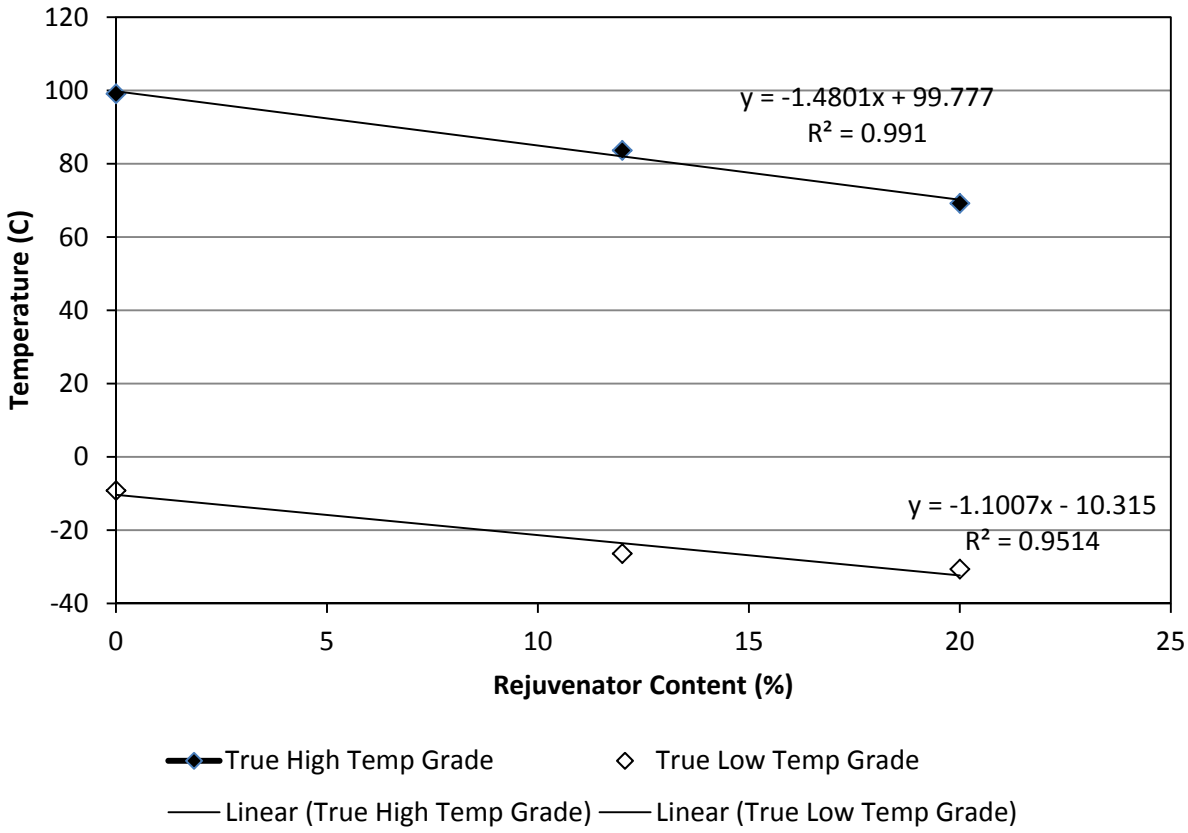

Property	Rejuvenator Content		
	0	12	20
High Temp DSR	99.1	83.6	69.2
Intermediate Temp DSR	33.1	22.1	18.0
Bending Beam Rheometer - S	-24.2	-30.7	-30.6
Bending Beam Rheometer - m	-9.2	-26.4	-31.2
True Grade	99.1 - 9.2	83.6 - 26.4	69.2 - 30.6
PG Grade	94 - 4	82 - 22	64 - 28

Figure 2 Effect of Rejuvenator Contents on RAP Binder

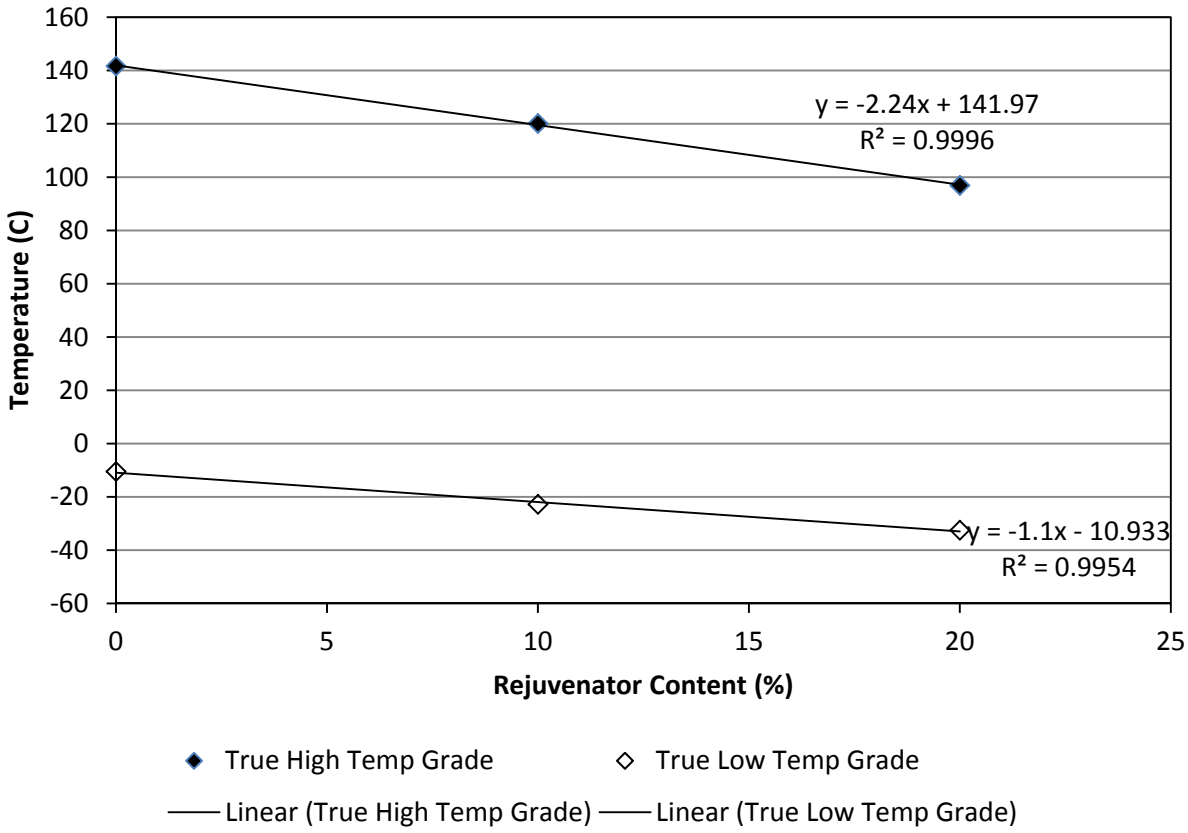

Property	Rejuvenator Content		
	0	10	20
High Temp DSR	141.7	120.1	96.9
Intermediate Temp DSR	34.1	24.0	14.9
Bending Beam Rheometer - S	-28.0	-30.9	-40.5
Bending Beam Rheometer - m	-10.5	-22.8	-32.5
True Grade	141.7 - 10.5	120.1 – 22.8	96.9 - 32.5
PG Grade	136 - 4	118 - 22	94 - 28

Figure 3 Effect of Rejuvenator Contents on RAS Binder

4.2 Mix Design

As previously mentioned, the five mixtures evaluated in this study were based on three mix designs. The control HMA mixture is a 9.5 mm dense-graded mix. The two mixtures with RAP—50% RAP mix and 50% RAP mix with rejuvenator—were based on the second 9.5 mm dense-graded mix design that contained 50% RAP by weight of aggregate. The two mixes with RAP and RAS—20% RAP plus 5% RAS mix and 20% RAP plus 5% RAS mix with rejuvenator—was based on the third 9.5 mm dense-graded mix design that contained 20% RAP and 5% RAS by weight of aggregate. Table 4 through Table 6 show the design gradations of the

three mix designs—the control, 50% RAP, and 20% RAP plus 5% RAS mix designs. Table 7 shows the consensus properties for the aggregate, RAP and RAS materials used in this study.

Table 4 Aggregate Gradation for Control Mix

Sieve Size (mm)	Sieve Size (Inches)	Percent Passing				
		Columbus Granite 89's	EAP Limestone 8910's	Columbus Granite M10's	Shorter Natural Sand	Total Blend
12.5	1/2"	100	100	100	100	100
9.5	3/8"	100	100	100	100	100
4.75	# 4	35	100	99	99	75
2.36	# 8	3	97	86	92	59
1.18	# 16	2	67	65	75	45
0.600	# 30	2	52	47	46	30
0.300	# 50	2	32	31	12	17
0.150	#100	2	22	20	2	10
0.075	#200	1.6	16.8	10.6	0.7	5.9
Cold Feed		**36%**	**15%**	**18%**	**31%**	

Table 5 Aggregate Gradation for 50% RAP Mix Design

Sieve Size (mm)	Sieve Size (Inches)	Percent Passing			
		Columbus Granite 89's	Shorter Natural Sand	RAP	Total Blend
12.5	1/2"	100	100	100	100
9.5	3/8"	99	100	99	100
4.75	# 4	32	100	83	74
2.36	# 8	5	89	64	56
1.18	# 16	3	70	50	43
0.600	# 30	2	39	35	28
0.300	# 50	3	14	22	15
0.150	#100	1	4	15	9
0.075	#200	0.8	0.8	9.5	5.1
Cold Feed		**25**	**25**	**50**	

Table 6 Aggregate Gradation for 20% RAP Plus 5% RAS Mix Design

Sieve Size (mm)	Sieve Size (Inches)	Percent Passing					
		Columbus Granite 89's	EAP Limestone 8910's	Shorter Natural Sand	RAP	RAS	Total Blend
12.5	1/2"	100	100	100	100	100	100
9.5	3/8"	100	100	100	99	99	100
4.75	# 4	32	99	100	83	95	72
2.36	# 8	5	90	89	64	93	55
1.18	# 16	3	65	70	50	73	42
0.600	# 30	2	48	39	35	53	27
0.300	# 50	3	36	14	22	46	15
0.150	#100	1	28	4	15	36	9
0.075	#200	0.8	20.2	0.8	9.5	24.1	5.6
Cold Feed		**35**	**10**	**30**	**20**	**5**	

Table 7 Consensus Aggregate Properties

Consensus Property	Columbus Granite 89's	EAP Limestone 8910's	Columbus Granite M10's	Shorter Natural Sand	RAP	RAS
Bulk Specific Gravity (Gsb)	2.610	2.819	2.707	2.614	2.708	2.723
Absorption (%)	1.5	0.5	0.3	0.2	0.5	0
Crushed Face Percentage	100	N/A	N/A	N/A	NA	N/A
FAA (Uncompacted Void Content)	N/A	48.4	50.2	45.8		
Sand Equivalency (%)	N/A	78	72	81		
Flat and Elongated Particle (%)	0	N/A	N/A	N/A	NA	N/A

The three mixtures were designed in accordance with AASHTO T323-07, AASHTO R35-09, AASHTO MP15-09, and AASHTO PP53-09, except that the N_{des} was 60 gyrations. The virgin binder used in the control mix was a PG 67-22. Table 8 summarizes the volumetric properties of the five mixtures tested in this study.

Table 8 Summary of Mixture Constituents and Volumetric Properties

Mix	Virgin	50%RAP	50%RAP + RA	20%RAP + 5%RAS	20%RAP + 5%RAS + RA
NMAS	9.5	9.5	9.5	9.5	9.5
Ndes	60	60	60	60	60
Total AC, %	6.1	6.2	6.5	6.2	6.4
V. AC, %	6.1 (100%*)	3.5 (56%*)	3.5 (54%*)	4.5 (72%*)	4.5 (71%*)
RA**, %			0.3 (4%*)		0.2 (3%*)
RAP AC, %		2.7 (44%*)	2.7 (42%*)	1.1 (18%*)	1.1 (17%*)
RAS AC, %				0.6 (10%*)	0.6 (9%*)
Gmb	2.369	2.361	2.348	2.351	2.353
Gmm	2.468	2.459	2.446	2.449	2.451
Va, %	4	4	4	4	4
VMA, %	16.5	16.9	17.6	17.2	16.9
VFA, %	75.4	75.7	77	76.2	77.2
DP	1.1	0.9	0.9	0.9	1
Eff. AC, %	5.4	5.6	5.9	5.7	5.7

*Based on total AC; **Rejuvenator-12% by total weight of recycled binders

For the RAS mix design, 100% blending was not assumed for the RAS binder in accordance with AASHTO PP 53-09. Based on the control mix design, a trial RAS mix design was performed to determine the initial optimum AC content to get the 4% design air voids. The data from the trial mix design were used to calculate the shingle binder availability factor (Equation 1) or the percentage of the RAS binder contributing to the final blended binder based on a procedure outlined in AASHTO PP 53-09. The shingle binder availability factor was 73.1% for the RAS used in this study. The binder content of the RAS was then adjusted using this factor for the final mix design.

$$F = 100\left(\frac{1+F_c}{2}\right) \quad (1)$$

$$F_c = \frac{(P_{bv}-P_{bvr})}{(P_{sr})(P_{br})} \quad (2)$$

where:

- F = the shingle asphalt binder availability factor (%) – 73.1% for this project
- F_c = the estimated shingle asphalt availability factor (%) – 46.1% for this project
- P_{bv} = the design asphalt binder content of a mix without RAS (%) - 6.1% for this project
- P_{bvr} = the design asphalt binder content of the same new mix with RAS (%) – 5.7% for this project
- P_{sr} = the percentage of RAS in the new HMA expressed as a decimal – 0.05 for this project

P_{br} = the percentage of shingle asphalt binder in the RAS expressed as a decimal – 0.1734 for this project

4.3 Performance Properties of Binder Blends

Based on the properties of the five mixtures, the virgin binder and four binder blends, as shown in Table 2, were prepared and tested. This section discusses the performance grading and LAS results for each binder blend.

4.3.1 Performance Grading of Binder Blends

Detailed results of PG testing of the five binder blends are included in Appendix B. Table 9 summarizes the performance grades determined for the virgin binder, the four binder blends, and each component of the blends. The rejuvenator was able to restore the low-temperature performance grades of the 50% RAP blend (PG 79.9-21.2) and the 20% RAP plus 5% RAS blend (PG 79.9-21.3) to a certain degree; however, these blends barely failed the low critical temperature requirement for a PG 67-22.

Table 9 Summary of Performance Grades

Properties	Virgin	50%RAP	50%RAP + RA	20%RAP + 5%RAS	20%RAP + 5%RAS + RA
Virgin AC*	67.0 - 23.2	67.0 - 23.2	67.0 - 23.2	67.0 - 23.2	67.0 - 23.2
RAP*		99.1 - 9.2	99.1 - 9.2	99.1 - 9.2	99.1 - 9.2
RAS*				141.7 - 10.5	141.7 - 10.5
RA Used	No	No	Yes	No	Yes
Total Blend	67.0 - 23.2	85.2 - 18.2	79.9 - 21.2	84.3 - 19.4	79.9 - 21.3

*Performance grade of binder before blending with the rejuvenator

4.3.2 Cracking Resistance of Binder Blends

The cracking resistance of binder blends was determined according to the proposed LAS test. This section briefly describes the LAS test, followed by an analysis of test results. A more detailed description of the LAS test method is included in Appendix C.

The LAS test is an accelerated binder fatigue test that has been proposed to replace the current DSR intermediate temperature G*sinδ parameter. The LAS procedure uses cyclic loading with increasing load amplitude to accelerate damage. The LAS test can account for material damage resistance, pavement structure, and traffic loading. The end result is a prediction of binder fatigue life as a function of strain in the pavement.

The LAS test is conducted in the DSR and consists of two steps, both of which may be conducted using the same asphalt binder sample, and the total testing time is approximately 30 minutes. The first step includes a frequency sweep from 0.1 to 30 Hz at a strain level of 0.1%, which is chosen so as not to induce damage into the sample. The second steps comprises of a strain sweep test at a constant frequency of 10 Hz with linearly increasing strain amplitude from

0.1 to 30% to create damage in the sample. The test is performed on asphalt binder that has been aged in the rolling thin-film oven (RTFO) using the 8 mm plates currently available for DSR intermediate temperature testing. The test can be conducted at either the tested intermediate temperature grade of the asphalt binder or the climatic intermediate temperature at a location where the asphalt binder is to be used. All testing for this study was performed at 32.1°C which corresponds to the local climate intermediate temperature in Auburn, Alabama.

Analysis of the LAS data is performed using viscoelastic continuum damage (VECD) theory which is based on Schapery's theory of work potential to model damage growth. The analysis is conducted in two steps. First, the material constant (α) is determined using complex shear modulus (G*) and phase angle (δ) from the frequency sweep test. The constant is typically calculated as a function of the slope of a log-log plot of relaxation modulus versus time. However, in the LAS procedure, the material constant is determined based on a simplified procedure developed by Hintz et al. (*26*) in which the material constant is estimated using the slope, *m*, of a log-log plot of storage modulus (G* cos(δ)) versus frequency (Equation 3).

$$\alpha = 1 + \frac{1}{m} \tag{3}$$

The second step is to analyze data from the strain sweep test. At each strain level of the test, multiple readings of G*, δ, and oscillatory stress are recorded. These data are used to determine accumulated damage levels in the specimen and the C_0, C_1, and C_2 constants for determining the damage parameter (D_f) (Equation 4), which corresponds to a 35% reduction in the undamaged |G*|sinδ (represented by C_0).

$$D_f = (0.35\frac{C_0}{C_1})^{\frac{1}{C_2}} \tag{4}$$

Finally, the binder fatigue performance parameter (N_f) is calculated using Equation 5. N_f can be adjusted to account for differences in pavement structure by changing γ_{max}. Higher strain values may correspond to thinner pavements or heavier traffic loading while lower strain values may correspond to thicker pavements or lighter traffic loads.

$$N_f = A(\gamma_{max})^B \tag{5}$$

where:

γ_{max} = applied binder strain for a given pavement structure, dimensionless
B = -2

$$A = \frac{f\left(D_f\right)^k}{k\left(\pi\frac{I_D}{|G^*|}C_1C_2\right)^\alpha}|G^*|^{-\alpha}$$

where:

f = loading frequency (10Hz)
k = $1+(1-C_2)\alpha$
|G*| = average value of G* from the 0.1% applied strain interval, MPa.
I_D = average value of |G*| from the initial interval of 0.1% applied strain, MPa

The applied binder strain is estimated using the strain in the pavement layer multiplied by 50 (*26*). Binder fatigue parameters (N_f) for two binder strain levels of 2.5% and 5% (Table 10) corresponding to 500 and 1,000 microstrain in the pavement layer, which has been used by Hintz et al. (*26*) for analysis, are determined for this study.

Table 10 Applied Binder Strain Levels

Pavement Layer Strain Level	Binder Strain Level
500 microstrain (ms)	0.000500 x 50 *100% = 2.5%
1000 microstrain (ms)	0.001000 x 50 *100% = 5%

Figure 4 and Figure 5 show graphical and statistical comparisons of the binder fatigue parameters (N_f) for the 2.5% and 5% applied binder strain levels at 32.1°C, respectively. The following observations can be drawn from the two figures.

- At the lower strain level, the binder fatigue parameters for the virgin binder and the 20% RAP plus 5% RAS blend with rejuvenator are not statistically different; however, the difference is statistically significant at the higher strain level.
- The binder fatigue parameters for the 50% RAP blend with rejuvenator and the 20% RAP plus 5% RAS blend are not statistically different at both the strain levels.
- The 50% RAP blend has the lowest binder fatigue parameters at both the strain levels.
- The effect of the rejuvenator on the 20% RAP plus 5% RAS blend is more significant than on the 50% RAP blend.

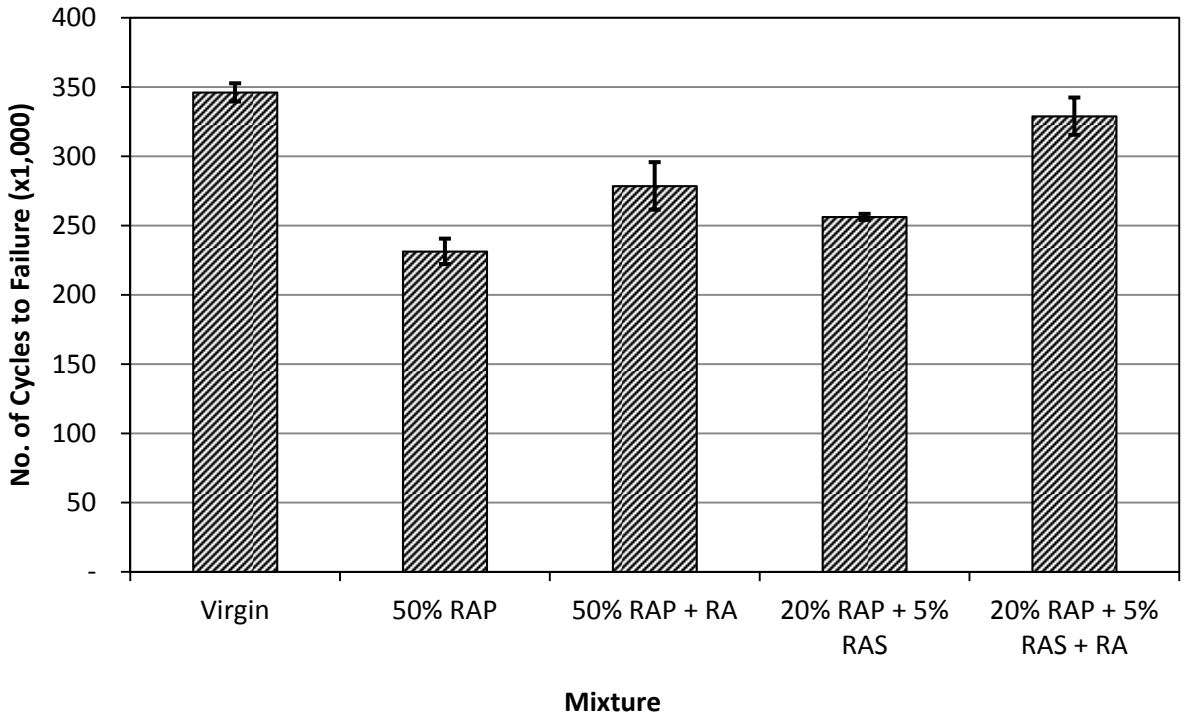

Statistical Analysis: No. of Cycles to Failure versus Binder Blend (shown in the above figure)

```
Factor  Type   Levels  Values
Blend   fixed       5  20% RAP + 5% RAS, 20% RAP + 5% RAS + RA, 50% RAP, 50%
                       RAP + RA, Virgin


Analysis of Variance for Fatigue Parameter, using Adjusted SS for Tests

Source  DF       Seq SS       Adj SS      Adj MS      F      P
Blend    4  18729400307  18729400307  4682350077  38.55  0.001
Error    5    607346203    607346203   121469241
Total    9  19336746511


S = 11021.3   R-Sq = 96.86%   R-Sq(adj) = 94.35%


Grouping Information Using Tukey Method and 95.0% Confidence

Blend                  N    Mean  Grouping
Virgin                 2  346126  A
20% RAP + 5% RAS + RA  2  328925  A
50% RAP + RA           2  278558    B
20% RAP + 5% RAS       2  256222    B C
50% RAP                2  231321      C

Means that do not share a letter are significantly different.
```

Figure 4 Binder Fatigue Parameters at Applied Binder Strain of 2.5%

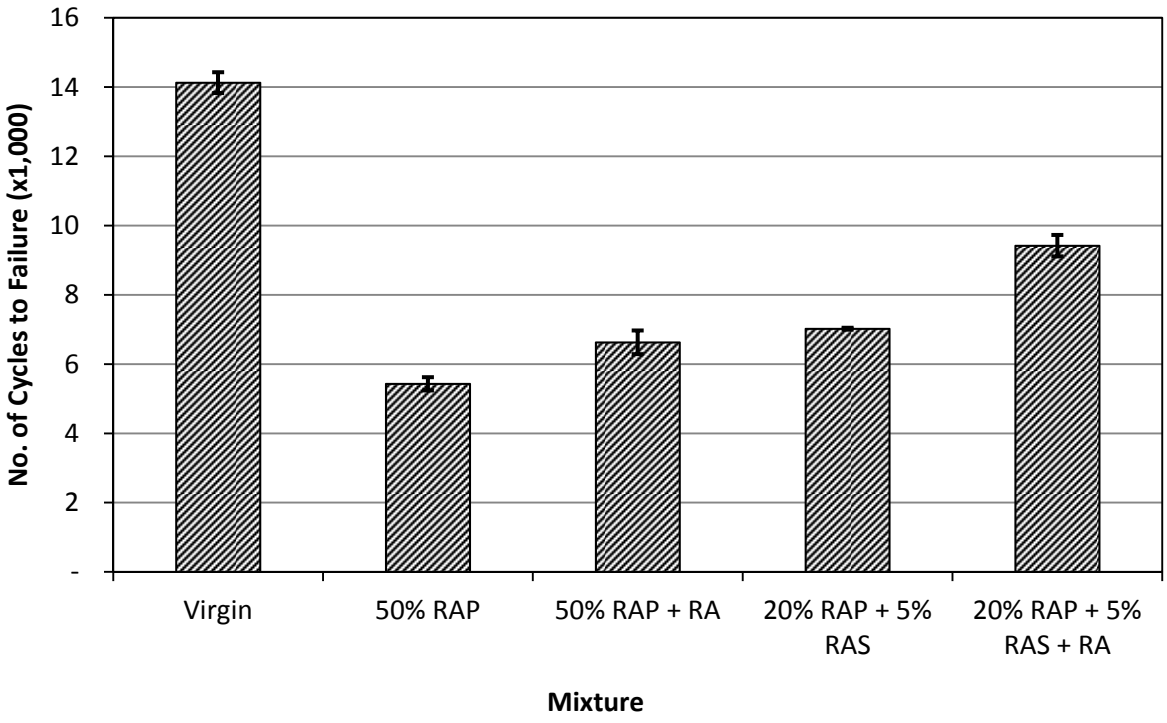

Statistical Analysis: No. of Cycles to Failure versus Binder Blend (shown in the above figure)

```
Factor  Type   Levels  Values
Blend   fixed       5  20% RAP + 5% RAS, 20% RAP + 5% RAS + RA, 50% RAP, 50%
                       RAP + RA, Virgin


Analysis of Variance for Fatigue Parameter, using Adjusted SS for Tests

Source  DF    Seq SS    Adj SS    Adj MS       F      P
Blend    4  95268953  95268953  23817238  351.41  0.000
Error    5    338884    338884     67777
Total    9  95607838


S = 260.340   R-Sq = 99.65%   R-Sq(adj) = 99.36%


Grouping Information Using Tukey Method and 95.0% Confidence

Blend                  N   Mean  Grouping
Virgin                 2  14127  A
20% RAP + 5% RAS + RA  2   9419    B
20% RAP + 5% RAS       2   7020      C
50% RAP + RA           2   6627      C
50% RAP                2   5429        D

Means that do not share a letter are significantly different.
```

Figure 5 Binder Fatigue Parameters at Applied Binder Strain of 5%

4.4 Performance Properties of Asphalt Mixtures

In this section, results of the following mixture tests are discussed:

- TSR test to evaluate moisture susceptibility
- E* test to evaluate stiffness of short-term and long-term aged mixtures
- ER and OT tests on long-term aged specimens to evaluate fracture resistance
- IDT test on long-term aged specimens to evaluate low-temperature cracking resistance
- APA test on short-term aged specimens to determine rutting resistance

All mixtures tested in this study were conducted using laboratory-prepared mixes. To prepare a sample in the laboratory, the aggregate was first carefully batched based on the design gradation. The aggregate, base binder, and RAP were heated to the mixing temperature (300^{o}F) in ovens. RAS was kept at the ambient temperature per specification. The liquid anti-strip agent was pre-blended in the base binder at its recommended dosage prior to mixing. If the rejuvenator was used in the mixture, it was also pre-blended in the base binder at the selected content of 12% by weight of recycled binder. After the aggregate, base binder, and RAP (if needed) had reached the mixing temperature, they were mixed in a mixing device. If RAS was used in the mixture, it was added to the mixture at the ambient temperature. The mixture was then short-term aged in an oven in accordance with the short-term aging procedure listed in AASHTO R30-02 or AASHTO T283-07 and compacted in a gyratory compactor. The compacted HMA specimens were then tested or long-term aged further in accordance with AASHTO R30-02 for testing.

4.4.1 Mixture Resistance to Moisture Damage

Moisture susceptibility testing was conducted in accordance with AASHTO T 283-07. Both the saturation and air void requirements specified in AASHTO T 283 were met for each specimen tested. Detailed results are presented in Appendix D.

Figure 6 compares the results of TSR test. The TSR values for all the mixtures tested in this study are equal or greater than the commonly accepted failure threshold of 0.8. The use of rejuvenator at the percentage used in the two RAP/RAS mixtures did not negatively affect the TSR values but slightly increased them.

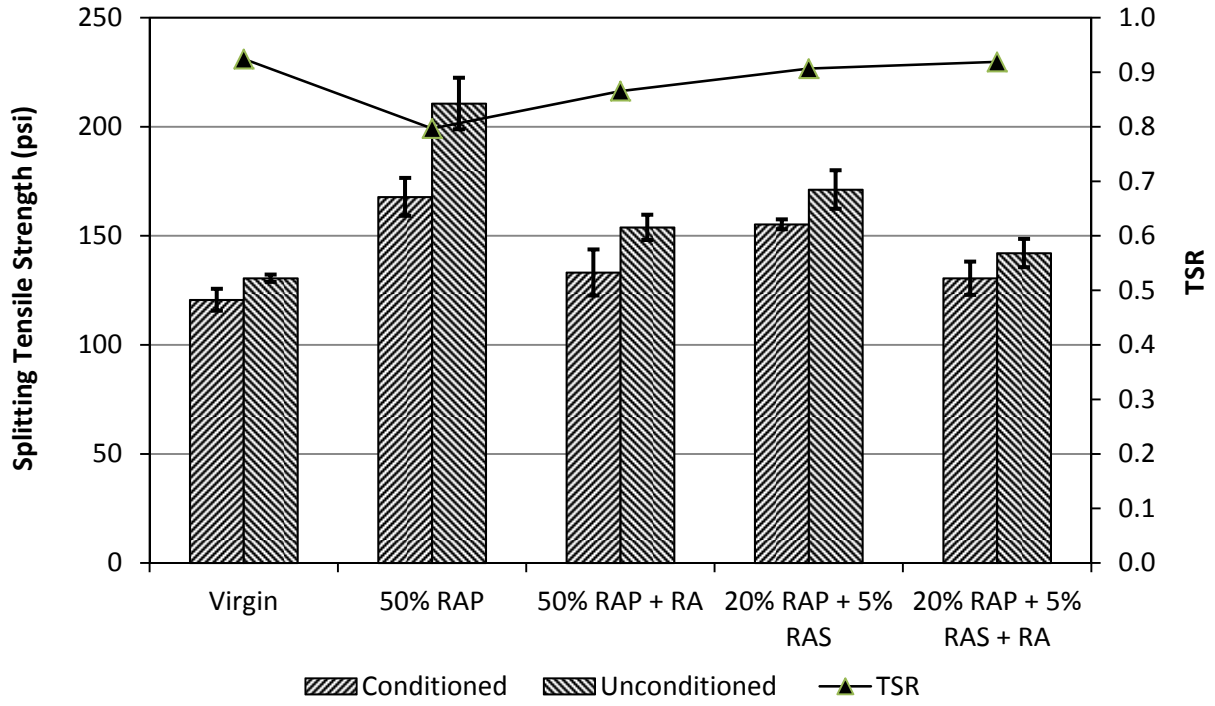

Figure 6 Comparison of TSR Testing Results

4.4.2 Mixture Stiffness

Dynamic modulus (E*) testing was conducted in accordance with AASHTO TP 79-09 on specimens that were prepared in accordance with AASHTO PP 60-09 to 7 ± 0.5 percent air voids. For each mix, two sets of three specimens were long-term and short-term aged and then tested to assess the effect of aging on the mixtures. The specimens were tested with the temperatures and frequencies recommended in AASHTO PP 61-09 using an IPC Global Asphalt Mixture Performance Tester (AMPT). Detailed results of E* testing are presented in Appendix E. Based on E* test results, mastercurves were generated in accordance with the procedure outlined in AASHTO PP 61-09 using the Mastersolver® program in EXCEL® developed under NCHRP 09-29. A reference temperature of 20^{o}C was used for this study. A detailed procedure regarding the dynamic modulus testing procedure and data analysis is documented in these specifications as well as in previous studies conducted at NCAT (*27*).

Figure 7 and Figure 8 compare the E* master curves at the reference temperature of 20^{o}C for the short-term and long-term aged specimens, respectively. For the short-term aged specimens, compared with the E* master curves of the 50% RAP and 20% RAP plus 5% RAS mixtures (without rejuvenator), the E* master curves for two mixes with rejuvenator are closer to that of the virgin mixture. However, for the long-term aged specimens, the two mixtures with rejuvenator appear to age faster than the other mixtures; the E* master curves of these mixtures are closer to those of the 50% RAP and 20% RAP plus 5% RAS mixtures without rejuvenator than to that of the virgin mix. The use of rejuvenator at the determined content in the two RAP/RAS mixtures softened the stiffness of these mixtures; however, these mixtures were still stiffer than the virgin mix.

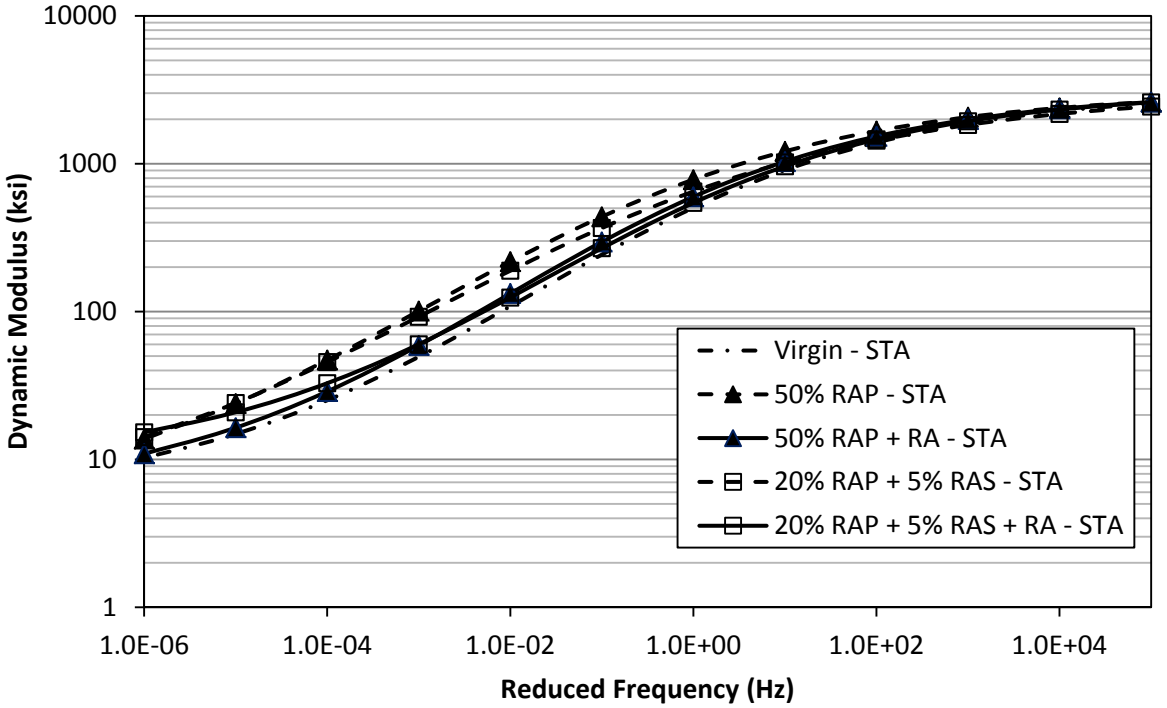

Figure 7 Comparison of E* Test Results for Short-Term Aged Specimens

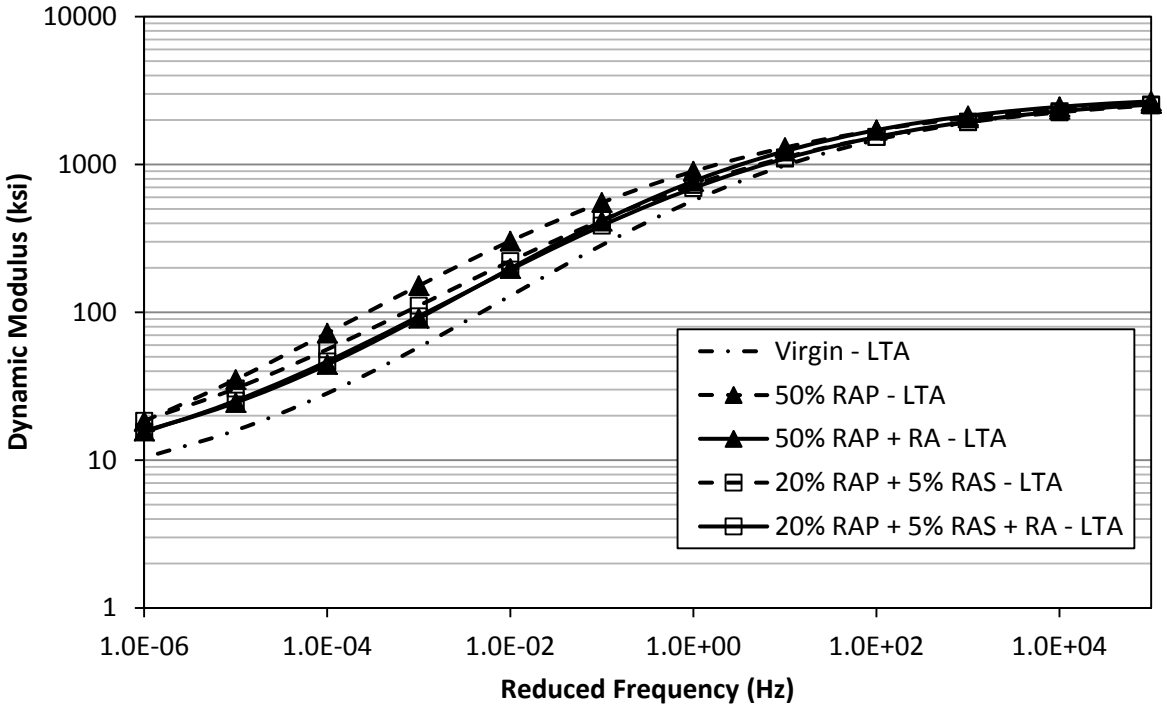

Figure 8 Comparison of E* Test Results for Long-Term Aged Specimens

4.4.3 Mixture Resistance to Top-Down Cracking

The resistance of the five asphalt mixtures to top-down cracking was evaluated using the energy ratio (ER) test procedure developed at the University of Florida (*28*). A brief description of the energy ratio test procedure is discussed below, followed by results of the ER test procedure for the five asphalt mixtures evaluated in this study.

Description of Energy Ratio Test Procedure. The ER test procedure includes three individual tests—resilient modulus, creep compliance, and indirect tensile strength. These tests are performed at 10°C using a universal testing device. Four specimens 150 mm in diameter by approximately 38 mm thick, cut from gyratory compacted samples, are used in the three tests. The target air voids for these samples are 7 ± 0.5%.

First, one specimen is used to determine appropriate loads for the resilient modulus and creep compliance tests. The target load for the resilient modulus test should produce a target horizontal strain of 100 to 200 μstrain on the specimen. The target load for the creep compliance test, which is usually approximately 10 percent of the load used in the resilient modulus test, should produce a horizontal strain of 100 μstrain after 100 seconds of testing. Then, for each of the remaining three specimens, the resilient modulus test is conducted in a load-controlled mode by applying the previously determined load (with a loading period of 0.1 seconds followed by a rest period of 0.9 seconds). The resilient modulus (M_r) is determined from the stress-strain curve (Figure 9a). After that, the target load for the creep compliance test is applied in a constant load control mode on the specimen for 1,000 seconds. The power function parameters (D_1 and *m*-value) are obtained by fitting the creep compliance curve to the test data (Figure 9b). Finally, the strength test is performed in a displacement-controlled mode at a loading rate of 2 in/min, much higher than the loading rate of 0.5 in/min used in the IDT strength test conducted according to AASHTO T322 to prevent creep at the higher test temperature. Figure 9c illustrates how the strength (St), fracture energy (FE), and dissipated creep strain energy at failure ($DCSE_f$) are determined from the stress-strain curves obtained from the strength and resilient modulus tests. Based on the data obtained from the three mixture tests and the tensile stress, ER can be determined using Equation 8 (*28*).

$$ER = \frac{DCSE_f}{DCSE_{min}} = \frac{DCSE_f \cdot \left[7.249 \cdot 10^{-5} \cdot \sigma^{-3.1}(6.36\text{-}St) + 2.46 \cdot 10^{-8}\right]}{m^{2.98} \cdot D_1} \quad (8)$$

where:

σ = tensile stress at the bottom of the asphalt layer, assumed 150 psi
M_r = resilient modulus
D_1, m = power function parameters
S_t = tensile strength
$DCSE_f$ = dissipated creep strain energy at failure
$DCSE_{min}$ = minimum dissipated creep strain energy required

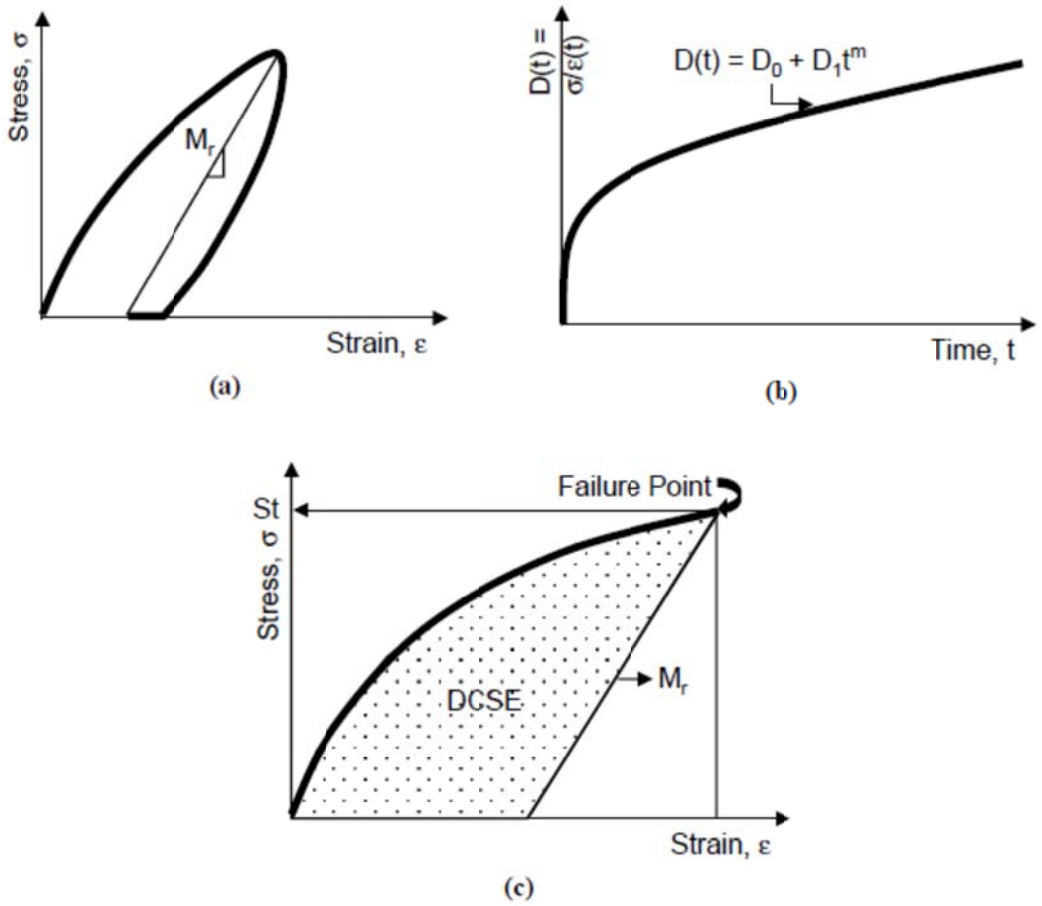

Figure 9 Parameters Determined from (a) Resilient Modulus, (b) Creep Compliance, and (c) Strength Tests (*29*)

An asphalt mixture with higher values of FE, $DCSE_f$, $DCSE_{min}$, and ER would have better resistance to top-down cracking. Based on an extensive study (*28*) performed on 22 field test sections gathered from cracked and uncracked sections throughout Florida to evaluate top-down cracking performance, the following criteria were recommended for evaluating the top-down cracking performance of asphalt mixtures.

- The dissipated creep strain energy threshold should be greater than 0.75 KJ/m^3.
- The minimum ER should be varied based on the traffic level, as shown in Table 11.

Table 11 Recommended Ratio Requirements (*28*)

Traffic (ESALs/year)	Minimum Energy Ratio (ER)
up to 250,000	1
250,001 to 500,000	1.3
500,001 to 1,000,000	1.95

Results and Analysis. Detailed results of the ER evaluation are presented in Appendix F. Figure 10 through Figure 13 compare the fracture properties—fracture energy, dissipated creep strain energy at failure, minimum dissipated creep strain energy, and energy ratio—for the five mixtures evaluated in this study. The following observations can be drawn from the plots.

- The trends shown in the plots for FE and $DCSE_f$ are similar, but they are slightly different from those of the plots for $DCSE_{min}$ and ER.
- Based on the FE and $DCSE_f$ plots, the virgin mix has the best resistance to top-down cracking, followed by the two 20% RAP plus 5% RAS mixes and then the 50% RAP mix with rejuvenator. The 50% RAP mix has the lowest resistance to top-down cracking.
- Based on the $DCSE_{min}$ plot, the 20% RAP plus 5% RAS mix with rejuvenator has the best resistance to top-down cracking, followed by the virgin mix, 20% RAP plus 5% RAS mix, 50% RAP mix with rejuvenator, and 50% RAP mix.
- However, based on the ER plot, the ranking is slightly different—the 20% RAP plus 5% RAS mix with rejuvenator exhibited lower resistance to top-down cracking than the 20% RAP plus 5% RAS mix without rejuvenator and the 50% RAP mix with rejuvenator.

In summary, the use of rejuvenator improved all four fracture properties for the 50% RAP mix and the FE, $DCSE_f$, and $DCSE_{min}$ of the 20% RAP plus 5% RAS mix. All the mixes, except the 50% RAP mix without rejuvenator, meet the proposed minimum $DCSE_f$ and ER requirements.

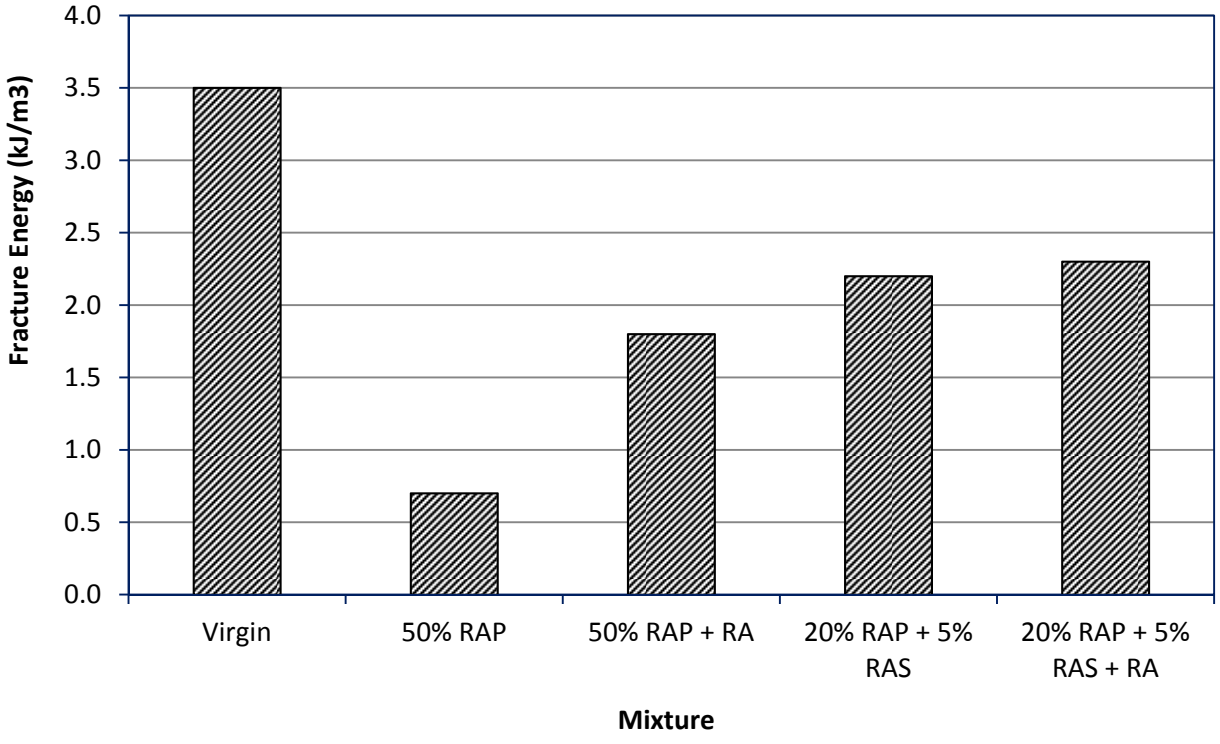

Figure 10 Fracture Energy

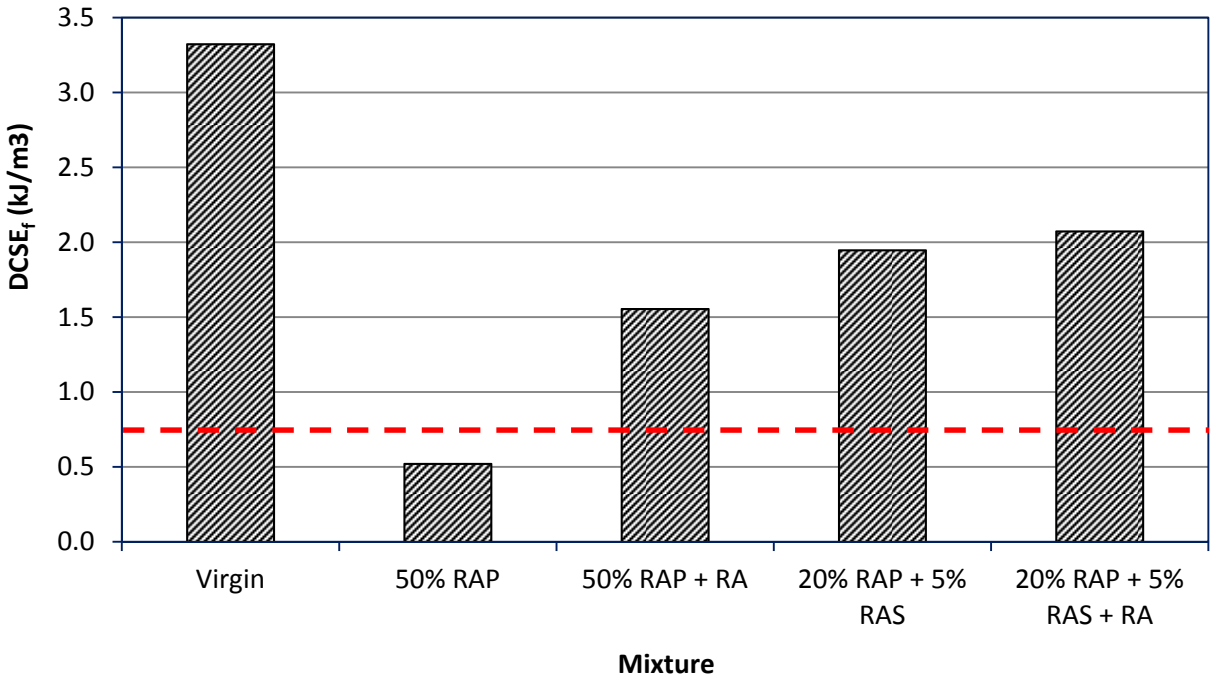

Figure 11 Dissipated Creep Strain Energy at Failure

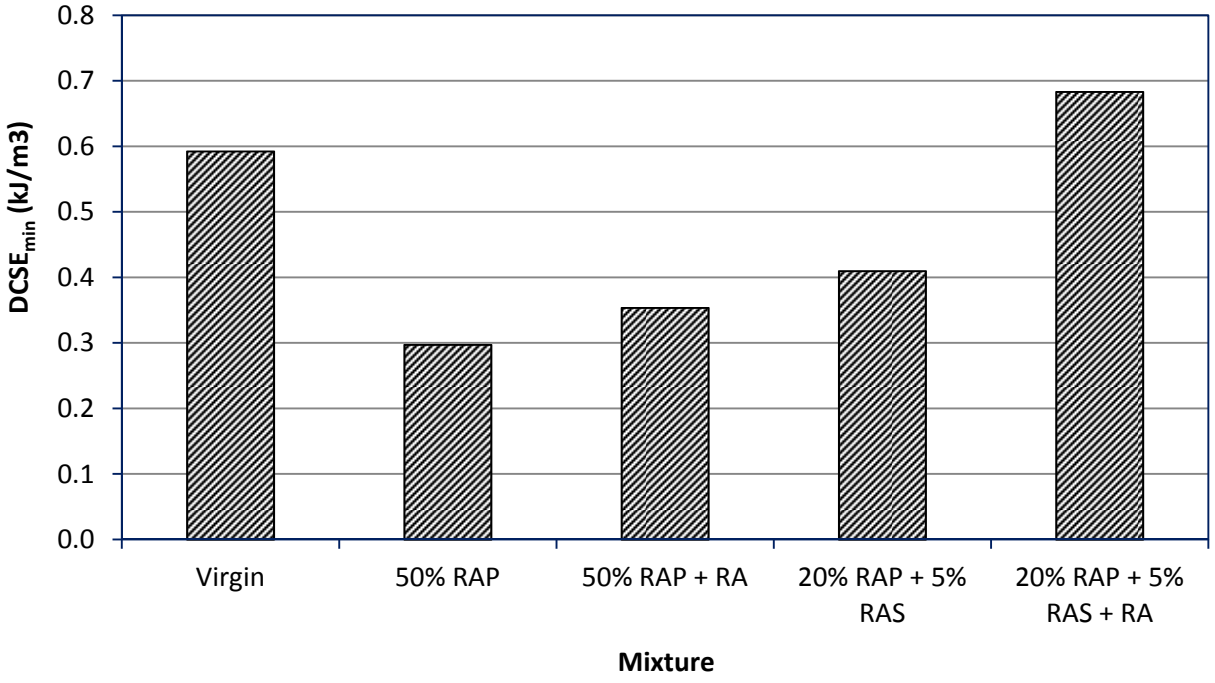

Figure 12 Minimum Dissipated Creep Strain Energy

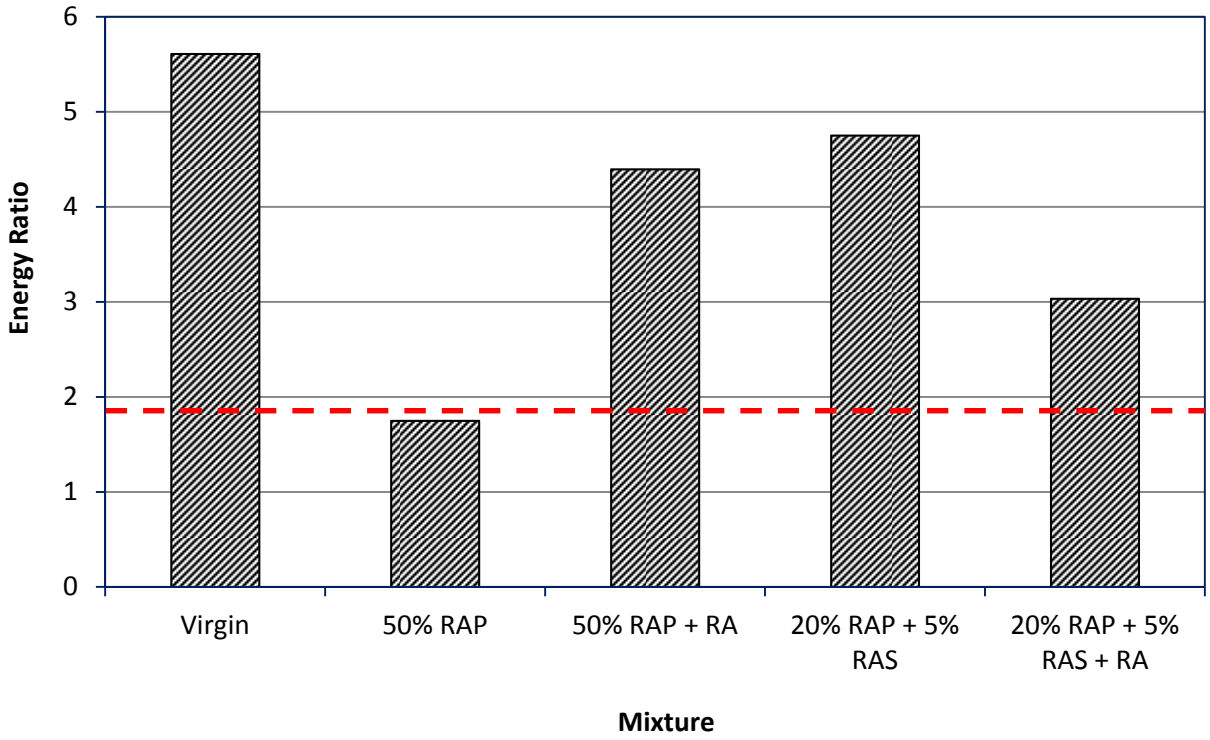

Figure 13 Energy Ratio

Table 12 shows the correlations between the parameters measured in the ER and LAS test procedures. It appears that the $DCSE_f$ is better correlated with the LAS results—N_f at 2.5% and 5% strain levels—than the ER. Figure 14 demonstrates the best correlation shown in Table 12 between the $DCSE_f$ and N_f at 5% strain.

Table 12 Correlation (R^2) between ER and LAS Results

ER Test Procedure	LAS Test Procedure	
	Nf @ 2.5% strain	Nf @ 5% strain
$DCSE_f$	0.75	0.87
Energy Ratio	0.27	0.40

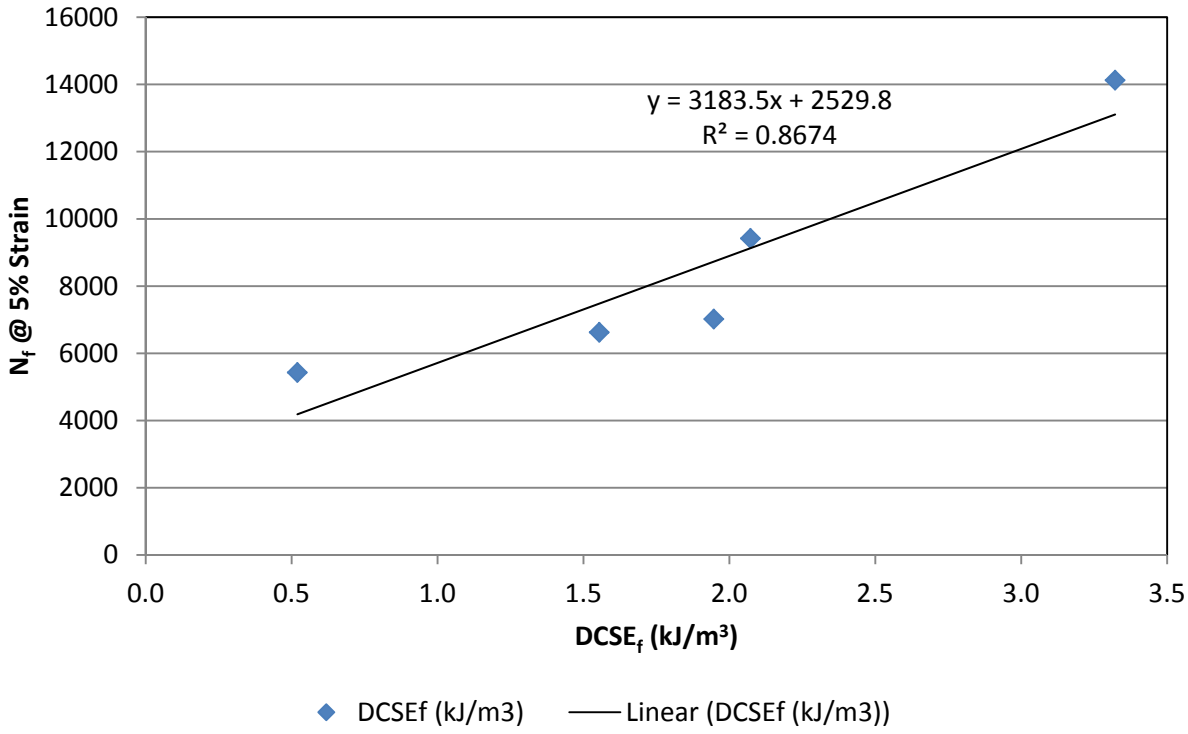

Figure 14 LAS N_f @ 5% Strain versus $DCSE_f$

4.4.4 Mixture Resistance to Low-Temperature Cracking

The resistance of the five mixtures to low-temperature cracking was evaluated using the IDT test procedure in accordance with AASHTO T 322-07. The test procedure includes two individual tests to measure creep compliance of each mixture at three temperatures—0, -10, and -20°C—and tensile strength at -10◦C. Four specimens were prepared for each mix. The first specimen was used to find a suitable creep load for that particular mix at each testing temperature. The remaining three specimens were tested at this load for data analysis. Specimens used for the creep and strength tests were 38 to 50 mm thick and 150 mm in diameter. Specimens were prepared to 7 ± 0.5% air voids.

Detailed results of the creep compliance and tensile strength tests are included in Appendix G. The results were used to determine the critical cracking temperature for each mix tested in this study. A brief description of each step of the analysis follows. A complete description of the thermal stress analysis can be found elsewhere (*30*, *31).*

Determination of Shift Factors and Prony Series. Theoretical and experimental results indicate that for linear visco-elastic materials, the effect of time and temperature can be combined into a single parameter through using the time-temperature superposition principle. From a proper set of creep compliance tests under different temperature levels, the creep compliance master curve can be generated by shifting the creep compliance data to a curve based on a reference temperature. This reference temperature is typically the lowest creep compliance

test temperature (-20°C for this study). The relations between real time t, reduced time ξ, and a shift factor a_T are given in Equation 9.

$$\xi = \frac{t}{a_T} \tag{9}$$

An automated procedure to generate the master curve was developed as part of the Strategic Highway Research Program (SHRP) *(32)*. The system requires measuring creep compliance test data at three different test temperatures. The final products of the system are a generalized Maxwell model (or Prony series), which is several Maxwell elements connected in parallel, and temperature shift factors. The generalized Maxwell model and shift factors are used for predicting thermal stress development of the asphalt mixture due to temperature change.

Linear Coefficient of Thermal Contraction. In addition to thermo-mechanical properties, it is required to estimate the thermal coefficient of the asphalt mixture for the critical temperature analysis. The thermal coefficient, α, for each asphalt mixture was estimated using Equation 10, which is a modified version of the relationship proposed by Jones et al. *(33)*.

$$\alpha = \frac{VMA * B_{AC} + V_{AGG} * B_{AGG}}{3 * V_{TOTAL}} \tag{10}$$

where:

α = linear coefficient of thermal contraction of the asphalt mixture (1/°C)
B_{AC} = volumetric coefficient of thermal contraction of the asphalt cement in the solid state (3.45 x 10^{-4}/°C)
B_{AGG} = volumetric coefficient of thermal contraction of the aggregate (1x10^{-6}/°C)
VMA = percent volume of voids in the mineral aggregate
V_{AGG} = percent volume of aggregate in the mixture
V_{TOTAL} = 100%

Thermal Stress and Critical Temperature Analyses. Based on the above parameters, the change in thermal stress for each mixture was estimated at the cooling rate of 10°C per hour, starting at 20°C. The finite difference solution developed by Soules et al. *(34)* was used to estimate thermal stress development based on the Prony Series coefficients (Equations 11 and 12). This analysis was performed in a MATHCAD program.

$$\sigma_i(t) = e^{-\Delta\xi/\lambda_i}\sigma_i(t - \Delta t) + \alpha \cdot \Delta T\, E_i \frac{\lambda_i}{\Delta\xi}\left(1 - e^{-\Delta\xi/\lambda_i}\right) \tag{11}$$

$$\sigma(t) = \sum_{i=1}^{N+1} \sigma_i(t) \tag{12}$$

where:

σ = thermal stress
ΔT and $\Delta\xi$ = changes in temperature and reduced time over the small time Δt.

Results and Analysis. Figure 15 shows thermal stress development as a function of a reduction in temperature. Figure 16 shows the critical temperatures determined at the points where thermal stresses exceed the tensile strengths.

Based on the results in Figure 15, at temperatures below -10◦C, the 50% RAP mixture appears to develop thermal stress more quickly than the other mixtures tested in this study, resulting in the highest critical failure temperature (-19.4°C). For the other mixtures, the thermal stresses are similar for temperatures below -20°C. As shown in Figure 16, the control mixture exhibits the lowest critical failure temperature (-27.7°C), followed by the 50% RAP mixture with rejuvenator, then the 20% RAP plus 5% RAS mix with rejuvenator, and finally the 20% RAP plus 5% RAS mix (without rejuvenator). A mix with a lower critical failure temperature would have better resistance to low-temperature cracking.

Figure 17 demonstrates a good correlation between the critical low temperatures determined using the IDT and BBR tests. While the critical low temperatures are not the same from the mix and binder tests, the ranking of the mixtures is similar to that of the binders in terms of their resistance to low-temperature cracking.

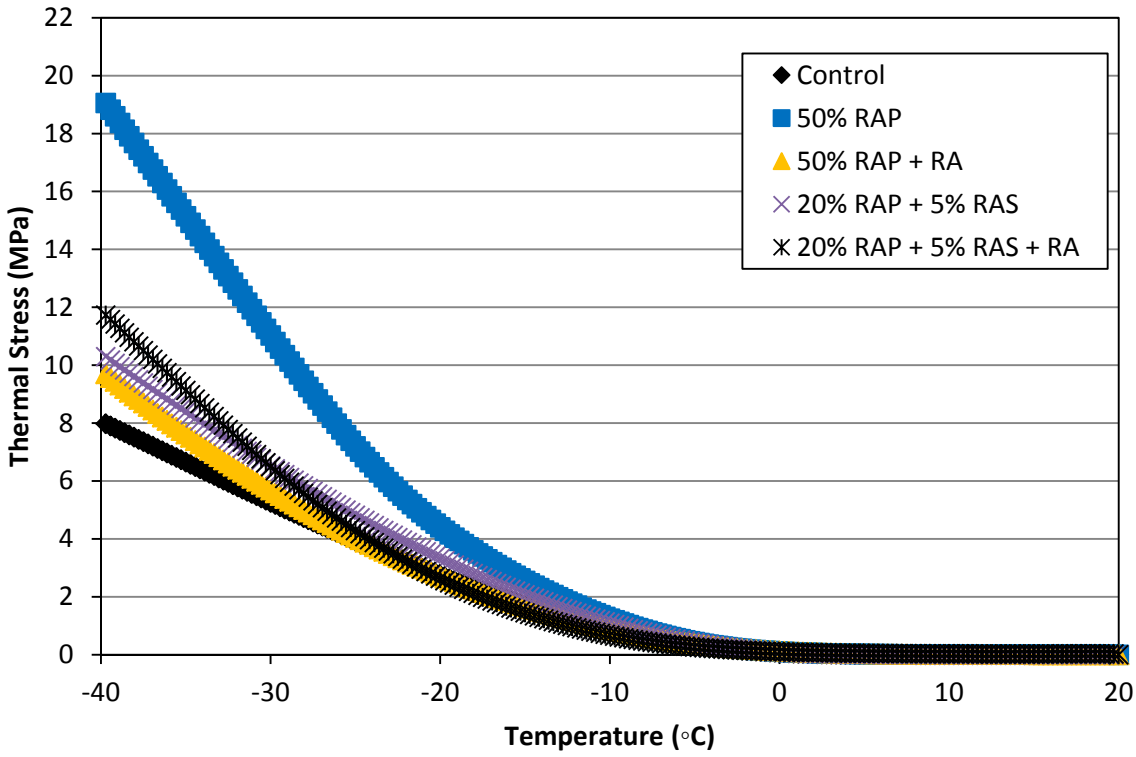

Figure 15 Thermal Stress versus Temperature

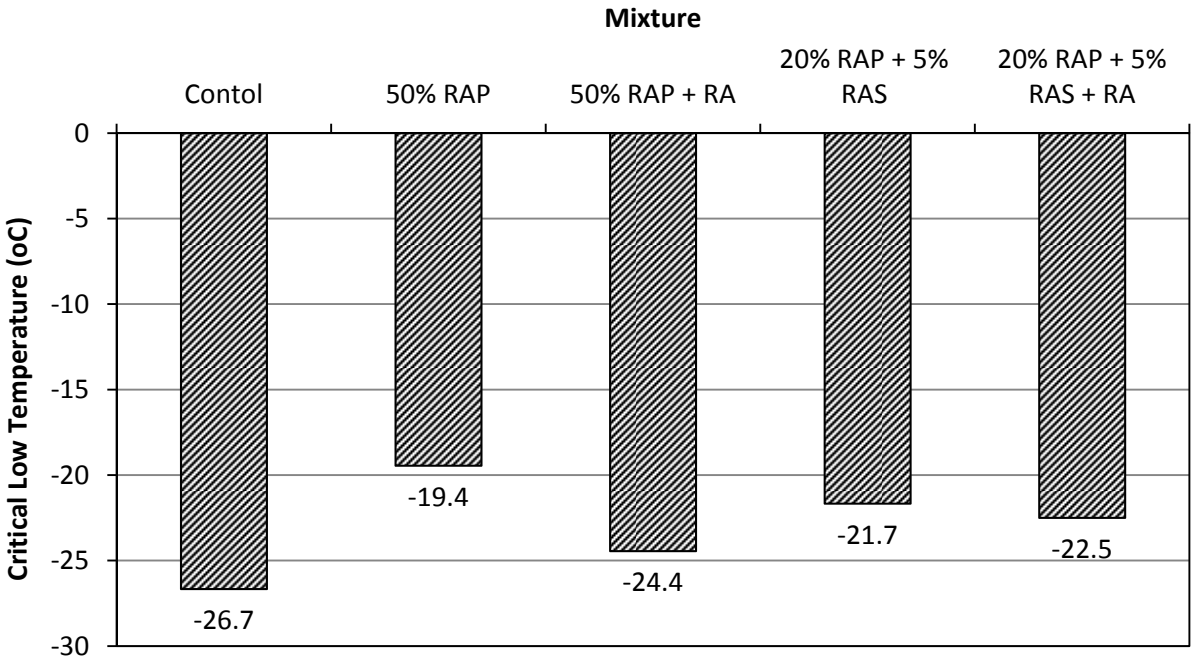

Figure 16 Critical Low Temperatures

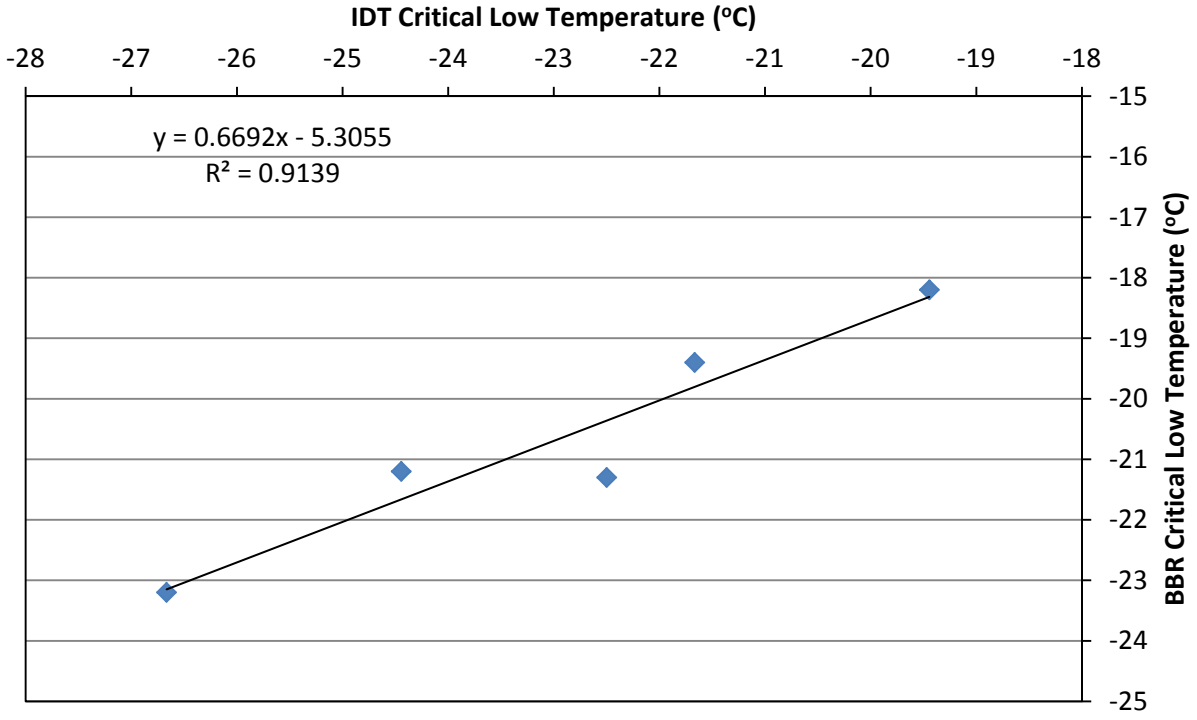

Figure 17 IDT versus BBR Critical Low Temperatures

4.4.5 Mixture Resistance to Reflective Cracking

The resistance of the five mixtures to reflective cracking was evaluated using the OT procedure in accordance with TxDOT 248-F, except that the maximum displacement per cycle was 0.013 in. instead of 0.025 in. The OT test was designed to simulate the reflective cracking of an asphalt concrete overlay atop a jointed Portland cement concrete (PCC) pavement. According to the TxDOT 248-F procedure, three replicate specimens of 6 in. long, 3 in. wide, and 1.5 in. high, which can be trimmed from a laboratory-compacted specimen of 6 in. in diameter and 4.5 in. in height or from a field core of 6 in. in diameter, should be tested for each mix. The target air void content of the test specimen prepared from a laboratory-compacted specimen is 7±1%. In this study, three replicates were tested for each mixture. The specimens were tested as 25°C in controlled displacement mode according to TxDOT 248-F. Loading with a saw-tooth waveform was applied at a rate of one cycle every 10 sec. The maximum load the specimen resisted in controlled displacement mode was recorded for each cycle. The test continued until sample failure, which is defined as a 93% reduction in load magnitude from the first cycle in the Tex 248-F procedure.

Detailed results of the overlay testing are included in Appendix H. Figure 18 shows graphical and statistical comparisons of the number of cycles to failure determined in the overlay testing. The virgin mix has the highest average number of cycles to failure, followed by the 20% RAP plus 5% RAS mix with rejuvenator, 50% RAP mix with rejuvenator, 20% RAP plus 5% RAS mix, and 50% RAP mix. However, in the statistical analysis, when considering the variability of the overlay test results, the difference in the number of cycles to failure between the recycled mixtures is not statistically significant, but the difference between the number of cycles to failure for the virgin mixture and those of the recycled mixtures is statistically significant.

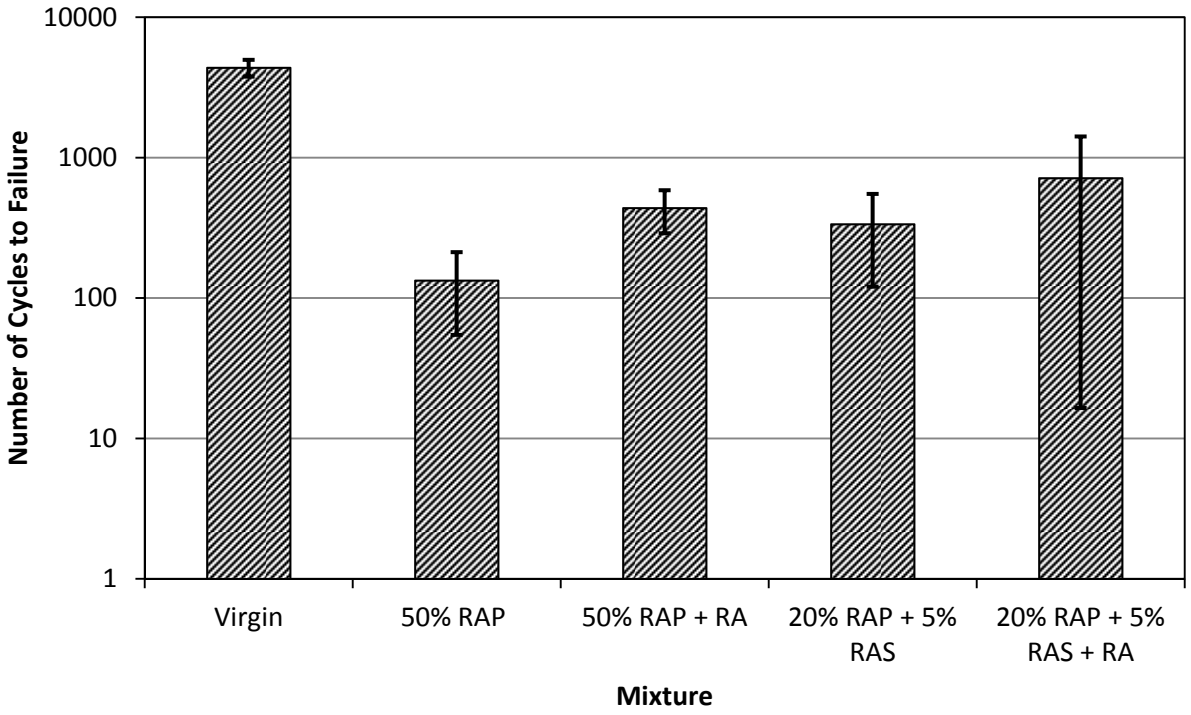

Statistical Analysis: No. of Cycles to Failure versus Mixture (shown in the above figure)

```
Factor  Type   Levels  Values
Mix ID  fixed       5  20% RAP + 5% RAS, 20% RAP + 5% RAS + RA, 50% RAP, 50%
                       RAP + RA, Virgin


Analysis of Variance for No. of Cycles to Failure, using Adjusted SS for Tests

Source  DF    Seq SS    Adj SS   Adj MS      F      P
Mix ID   4  38222841  38222841  9555710  51.97  0.000
Error   10   1838775   1838775   183878
Total   14  40061616

S = 428.809   R-Sq = 95.41%   R-Sq(adj) = 93.57%


Grouping Information Using Tukey Method and 95.0% Confidence

Mix ID                 N    Mean  Grouping
Virgin                 3  4368.3  A
20% RAP + 5% RAS + RA  3   714.7    B
50% RAP + RA           3   437.3    B
20% RAP + 5% RAS       3   335.3    B
50% RAP                3   133.3    B

Means that do not share a letter are significantly different.
```

Figure 18 Comparison of Overlay Tester Results

4.4.6 Mixture Resistance to Permanent Deformation

The rutting resistance of the five mixtures was evaluated using an Asphalt Pavement Analyzer (APA) in accordance with AASHTO T340-10. The specimens used for this testing were prepared to a height of 75 mm and an air void level of 7 ± 0.5 percent. Six replicates were tested for each mix. The samples were tested at a temperature of 64°C (the 98% reliability temperature for the high PG grade of the binder in Opelika, Alabama). The samples were loaded by a steel wheel (loaded to 100 lbs) resting on a pneumatic hose pressurized to 100 psi for 8,000 cycles. Manual depth readings were taken at two locations on each specimen before and after the loading was applied to determine the specimen rut depth. Automatic depth measurements were also recorded for comparison.

A summary of APA testing results is included in Appendix I. Figure 19 graphically and statistically compares the average values and variability of the manually and automatically measured rut depths for the five mixtures. It can be seen that the two mixtures with rejuvenator have higher manually measured APA rut depths than the control mix and the 20% RAP plus 5% RAS mix without rejuvenator. The 50% RAP mix without rejuvenator has the lowest APA rut depth. Statistically, there are three groups of mixtures that have significantly different rut depths. The first group with the highest rut depths includes the two mixtures with rejuvenator. The second group consists of three mixtures—20% RAP plus 5% RAS with rejuvenator, control, and 20% RAP plus 5% RAS (without rejuvenator). The last group includes only the 50% RAP mix.

A past study at the NCAT Pavement Test Track has shown that if a mixture has an average APA manual rut depth less than 5.5 mm, it should be able to withstand at least 10 million equivalent single axle loads (ESALs) of traffic at the test track without accumulating more than 12.5 mm of field rutting (*35*). Considering this threshold, all five mixtures are expected to pass in terms of rutting.

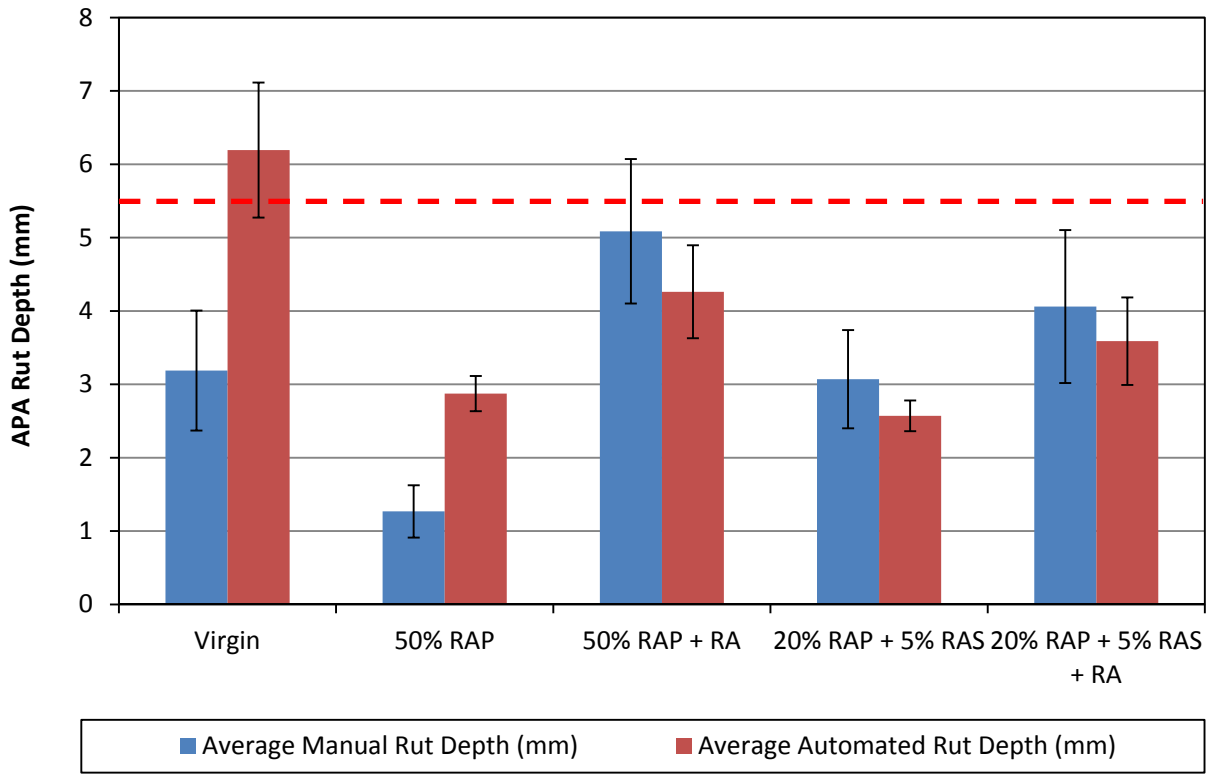

General Linear Model: Manual Rut versus Mix

```
Factor  Type   Levels  Values
Mix     fixed       5  20% RAP + 5% RAS, 20% RAP + 5% RAS + RA, 50% RAP, 50%
                       RAP + RA, Virgin


Analysis of Variance for Manual Rut (25-Final), using Adjusted SS for Tests

Source  DF  Seq SS  Adj SS  Adj MS      F      P
Mix      4  47.749  47.749  11.937  18.08  0.000
Error   25  16.509  16.509   0.660
Total   29  64.257

S = 0.812619   R-Sq = 74.31%   R-Sq(adj) = 70.20%


Grouping Information Using Tukey Method and 95.0% Confidence

Mix                   N   Mean  Grouping
50% RAP + RA          6  5.086  A
20% RAP + 5% RAS + RA 6  4.061  A B
Virgin                6  3.188    B
20% RAP + 5% RAS      6  3.071    B
50% RAP               6  1.268      C

Means that do not share a letter are significantly different.
```

Figure 19 Comparison of APA Testing Results

5 COST COMPARISON

Based on the mixture constituents shown in Table 8, a cost comparison was conducted, and the results are given in Table 13. Compared to the cost per ton of virgin mix, use of 50% RAP mix, 50% RAP mix with rejuvenator, 20% RAP plus 5% RAS mix, or 20% RAP plus 5% RAS mix with rejuvenator can save approximately 36, 29, 21, or 16 percent on materials cost per ton of mix, respectively.

Table 13 Cost Comparison

Component		Cost per ton of Material (USD)	Cost per ton of Mix (USD)				
			Virgin Mix	50% RAP	50% RAP + RA	20% RAP + 5% RAS	20% RAP + 5% RAS + RA
Binder	PG 67-22	600	36.6	21.0	21.0	27.0	27.0
	RAP AC***	0	0.0	0.0	0.0	0.0	0.0
	RAS AC*	25	0.0	0.0	0.0	0.2	0.2
	RA**	1200	0.0	0.0	3.6	0.0	2.4
Aggregate	Virgin Agg	15	14.1	7.0	7.0	11.2	11.2
	RAP Agg***	9	0.0	4.2	4.2	1.7	1.7
Total			50.7	32.3	35.9	40.1	42.5
Percent of Virgin Mix				63.6	70.7	79.2	83.9
Percent Savings				36.4	29.3	20.8	16.1

* Total RAS AC = effective RAS AC*100/73
** $4/gallon at facility in CA, $5/gallon at a plant in Alabama
*** Including costs for both RAP AC and RAP aggregate

6 CONCLUSIONS AND RECOMMENDATIONS

This study evaluated the effect of using rejuvenator on the mechanistic and performance properties of recycled binders and mixtures with high RAP and RAS contents in the laboratory. The testing plan for this study consisted of determining the optimum content for rejuvenator, mix design, and conducting binder and mixture tests to assess the performance characteristics (moisture susceptibility, mixture stiffness, top-down cracking, low-temperature cracking, and rutting) of the four recycled asphalt mixtures—50% RAP mix, 50% RAP mix with rejuvenator, 20% RAP plus 5% RAS mix, and 20% RAP plus 5% RAS mix with rejuvenator—relative to those of the control mixture. The following conclusions and recommendations are offered based on the results of this study.

- The desired amount of rejuvenator can be determined based on a linear relationship between the rejuvenator content and critical low temperature of the blend of recycled binder and rejuvenator. In this study, a rejuvenator content of 12% by the total weight of recycled binders was selected to restore the performance properties of the recycled binders to meet the requirements for a PG 67-22, which is the performance grade of the virgin binder.

- The mixtures evaluated in this study were designed in accordance with AASHTO T323-07, AASHTO R35-09, AASHTO MP15-09, and AASHTO PP53-09, except that the N_{des} was 60 gyrations. The rejuvenator was used in the recycled mixes to improve their resistance to cracking.
- The shingle binder availability factor or the percentage of the RAS binder contributing to the final blended binder was determined in accordance with AASHTO PP 53-09. The shingle binder availability factor was 73.1% for the RAS used in this study. The binder content of the RAS was then adjusted using this factor for the final mix design.
- The rejuvenator at a content of 12% by the total weight of recycled binders was able to restore the critical low temperature of (1) the blend of 50% RAP and virgin binder from -18.2 to -21.2 and (2) the blend of 20% RAP plus 5% RAS and virgin binder from -19.4 to -21.3. However, these blends barely failed the low critical temperature requirement for a PG 67-22.
- The cracking resistance of binder blends was evaluated based on the binder fatigue parameters (N_f) for the 2.5% and 5% binder strain levels determined at 32.1°C in accordance with the proposed LAS test. The virgin binder and the 20% RAP plus 5% RAS blend with rejuvenator had better resistance to fatigue cracking, followed by the 50% RAP blend with rejuvenator and the 20% RAP plus 5% RAS blend (without rejuvenator). The 50% RAP blend has the lowest binder fatigue parameters at both the strain levels. The effect of the rejuvenator on the 20% RAP plus 5% RAS blend is more significant than on the 50% RAP blend.
- The moisture resistance of the mixtures was evaluated using the TSR test. The TSR values for all the mixtures tested in this study were equal or greater than the commonly accepted failure threshold of 0.8. The use of rejuvenator at the determined content in the two RAP/RAS mixtures did not negatively affect the TSR values but slightly increased them.
- Dynamic modulus testing was conducted to evaluate the mixture stiffness. For each mix, two sets of specimens were long-term and short-term aged and then tested to assess the effect of aging on the mixtures. Based on the test results, the two mixtures with rejuvenator appeared to age faster than the other mixtures. The use of rejuvenator at the determined content in the recycled mixtures softened the stiffness of these mixtures; however, these mixtures were still stiffer than the virgin mix in both long- and short-term aged conditions.
- The resistance of the five asphalt mixtures to top-down cracking was evaluated using the energy ratio (ER) test procedure. The use of rejuvenator improved all the four fracture properties—FE, $DCSE_f$, $DCSE_{min}$ and ER—for the 50% RAP mix and the FE, $DCSE_f$ and $DCSE_{min}$ of the 20% RAP plus 5% RAS mix. All the mixes, except the 50% RAP mix without rejuvenator, meet the proposed minimum $DCSE_f$ and ER requirements.
- The analysis of the correlation between the parameters measured in the ER and LAS test procedures showed that the $DCSE_f$ was better correlated with the LAS results—N_f at 2.5% and 5% strain levels—than the ER.
- The resistance of the five mixtures to low-temperature cracking was evaluated using the IDT test procedure. The control mixture exhibits the lowest critical failure temperature (-27.7°C), followed by the 50% RAP mixture with rejuvenator, then the 20% RAP plus 5% RAS mix with rejuvenator, and the 20% RAP plus 5% RAS mix (without rejuvenator). A

mix with a lower critical failure temperature would have better resistance to low-temperature cracking.

- The critical low temperatures determined using the IDT correlated well with those determined using the BBR test. The ranking of the mixtures is similar to that of the binders in terms of their resistance to low-temperature cracking.
- The resistance of the five mixtures to reflective cracking was evaluated using the OT procedure in accordance with TxDOT 248-F, except that the maximum displacement per cycle is 0.013 in. instead of 0.025 in. The virgin mix has the highest average number of cycles to failure that is statistically different from those of the recycled mixes. Among the recycled mixtures, the 20% RAP plus 5% RAS mix with rejuvenator has the highest average number of cycles to failure, followed by 50% RAP mix with rejuvenator, 20% RAP plus 5% RAS mix, and 50% RAP mix; however, the differences in the number of cycles to failure among the recycled mixes are not statistically significant.
- The rutting resistance of the five mixtures was evaluated using the APA. All the mixtures exhibited APA manual rut depths less than 5.5 mm, which was determined based on the past research at the NCAT Pavement Test Track; thus, all five mixtures were not suspected to fail in terms of rutting.
- Based on a cost comparison, use of 50% RAP mix, 50% RAP mix with rejuvenator, 20% RAP plus 5% RAS mix, or 20% RAP plus 5% RAS mix with rejuvenator can provide cost savings of approximately 36, 29, 21, or 16 percent, respectively, compared to the cost per ton of virgin mix.

In summary, the use of rejuvenator in the recycled mixtures improved the cracking resistance of these mixtures without adversely affecting their resistance to moisture damage and permanent deformation. It is recommended that the rejuvenator, which is pre-blended with the virgin binder, be used to improve the cracking resistance of asphalt mixtures with high RAP and RAS contents. However, since the virgin binder pre-blended with the rejuvenator may be much softer than the normal grade of asphalt being used, good mixing of the binder pre-blended with the rejuvenator, aggregate, and recycled material is important to produce a good asphalt mixture that can avoid premature rutting failures. Further research should be conducted to evaluate other rejuvenators and the use of rejuvenator in asphalt mixtures with higher recycled contents and with tear-off RAS.

REFERENCES

1. Boomquist, D., G. Diamond, M. Oden, B. Ruth, and M. Tia. *Engineering and Environmental Aspects of Recycled Materials for Highway Construction.* Report No. FHWA-RD-088, FHWA, Washington, DC, 1993.
2. EPA. 1998. http://www.epa.gov/wastes/conserve/rrr/imr/cdm/pubs/roof_br.pdf. (accessed October 24, 2011).
3. McDaniel, R., H. Soleymani, M. Anderson, P. Turner, and R. Peterson. *Recommended Use of Reclaimed Asphalt Pavement in the SuperPave Mixture Design Method.* NCHRP Report 452, TRB, Washington, DC, 2000.
4. Mallick, R., M. Tao, K. O'Sullivan, and R. Frank. "Why Not (Use Rejuvenator For) 100% RAP Recycling?" *Proceedings of the 89th TRB Annual Meeting*, TRB, Washington, DC, 2010.
5. Thyrion, F. "Asphalt Oxidation," *Asphaltenes and Asphalts: Development in Petroleum Science*, Vol. 40B, Elsevier, NY, 2000, pp. 445-474.
6. Corbett, L. "Reaction Variables in the Air Blowing of Asphalt." *Industrial and Engineering Chemistry Process Design and Development,* Vol. 14, 1975, pp. 181-187.
7. Petersen, J. "Chemical Composition of Asphalt as Related to Asphalt Durability: State of the Art," *Transportation Research Record 999*, TRB, Washington, DC, 1984, pp. 13-30.
8. Roberts, F., P. Kandhal, E. R. Brown, D.Y. Lee, and T. Kennedy. *Hot Mix Asphalt Materials, Mixture Design and Construction,* 2nd Ed. NAPA, Lanham, MD, 1996.
9. Terrel, R., and J. Epps. "Using Additives and Modifiers in Hot-Mix Asphalt," *Quality Improvement Series (QIP 114 A)*, NAPA, Lanham, MD, 1989.
10. Bullin, J., R. Davison, C. Glover, J. Chaffin, M. Liu, and R. Madrid. *Development of Superior Asphalt Recycling Agents, Phase 1: Technical Feasibility.* Final Technical Progress Report DE97006951, Department of Energy, 1997.
11. Dunning, R., and R. Mendenhall. "Design of Recycled Asphalt Pavements and Selection of Modifiers," *Recycling of Bituminous Pavements,* ASTM STP 662, Ed. L. Wood, PA, 1978.
12. Lee, C., R. Terrel, and J. Mahoney. "Test for Efficiency of Mixing of Recycled Asphalt Paving Mixtures," *Transportation Research Record 911*, TRB, Washington, DC, 1983, pp. 51-60.
13. Carpenter, S., and J. Wolosick. "Modifier Influence in the Characterization of Hot-Mix Recycled Material," *Transportation Research Record 777*, TRB, Washington, DC, 1980, pp. 15-22.
14. Noureldin, S., and L. Wood. "Rejuvenator Diffusion in Binder Film for Hot-Mix Recycled Asphalt Pavement," *Transportation Research Record 1115*, TRB, Washington, DC, 1987, pp. 51-61.
15. Huang, B., G. Li, D. Vukosavljevic, X. Shu, and B. Egan. "Laboratory Investigation of Mixing Hot-Mix Asphalt with Reclaimed Asphalt Pavement," *Transportation Research Record 1929*, TRB, Washington, DC, 2005, pp. 37-45.
16. Karlsson, R. and U. Isacsson. "Investigations on Bitumen Rejuvenator Diffusion and Structural Stability," Journal of the Association of Asphalt Paving Technologists, Vol. 72, AAPT, Lino Lakes, MN, 2003, pp. 463-501.
17. Oliver, J. *Diffusion of oils in asphalts.* Report No. 9, Australian Road Research Board, Vermont South, Victoria, Australia, 1975.

18. Karlsson, R., and U. Isacsson. “Application of FTIR-ATR to Characterization of Bitumen Rejuvenator Diffusion,” *Journal of Materials in Civil Engineering*, Vol. 15, No. 2, ASCE, 2003.
19. Kadar, P. “Field and Laboratory Properties of Recycled Asphalt Pavement,” *Asphalt Review*, Australia, 1996, pp. 9-12.
20. Potter, J., and J. Mercer. “Full-Scale Performance Trials and Accelerated Testing of Hot-Mix Recycling in the UK.” *Proceedings of the 8th International Conference on Asphalt Pavements*, International Society for Asphalt Pavements, Seattle, 1997, 593–607.
21. Tam, K., P. Joseph, and D. Lynch. “Five-year experience of low-temperature performance of recycled hot mix,” *Transportation Research Record 1362*, TRB, Washington, DC, 1992, pp. 56–65.
22. Terrel, R., and D. Fritchen. “Laboratory Performance of Recycled Asphalt Concrete,” *ASTM STP 662*, L. E. Wood, ed., ASTM, Philadelphia, 1977, pp. 104–122.
23. DeKold, S., and S. Amirkhanian. “Reuse of Moisture Damaged Asphaltic Concrete Pavements.” *Transportation Research Record 1337*, TRB, Washington, DC, 1992, pp. 79–88.
24. Epps, J., D. Little, and R. Holmgreen. “Guidelines for recycling pavement materials.” *NCHRP Report No. 224*, TRB, Washington, DC, 1980.
25. National Lime Association (NLA). “How to Add Hydrated Lime to Asphalt: An Overview of Cureent Methods.” Accessed on April, 14th, 2011. (http://www.lime.org/documents/publications/free_downloads/how-to-add-lime.pdf)
26. Hintz, C., R. Velasquez, C. Johnson, H. Bahia. “Modification and Validation of the Linear Amplitude Sweep Test for Binder Fatigue Specification,” Submitted for publication and presentation at the Transportation Research Board Annual Meeting, Washington, D.C., January 2011.
27. Timm, David H., Mary M. Robbins, James R. Willis, Nam H. Tran, and Adam J. Taylor. *Evaluation of Mixture Performance and Structural Capacity of Pavements Utilizing Shell Thiopave - Phase II: Construction, Laboratory Evaluation and Full-Scale Testing of Thiopave Test Sections - One Year Report.* NCAT Report 11-03, Auburn Univeristy, Alabama, 2011.
28. Roque, R., B. Birgisson, C. Drakos, and B. Dietrich. "Development and Field Evaluation of Energy-Based Criteria for Top-down Cracking Performance of Hot Mix Asphalt." *Journal of the Association of Asphalt Paving Technologists, Vol 73*, 2004, pp. 229-260.
29. Timm, David H., Gregory A. Sholar, Jaeseung Kim, and J. Richard Willis. "Forensic Investigation and Validation of Energy Ratio Concept." *Transportation Research Record: Journal of the Transportation Research Board, No. 2127*, 2009: pp. 43-51.
30. Hiltunen, D. R. and R. Roque. “A Mechanics-Based Prediction Model for Thermal Cracking of Asphaltic Concrete Pavements.” *Journal of the Association of Asphalt Paving Technologists,* 63, 1994, pp. 81–117.
31. Kim, J., R. Roque, and B. Birgisson. “Integration of Thermal Fracture in the HMA Fracture Model.” *Journal of the Association of Asphalt Paving Technologists*, 77, 2008, pp. 631–662.
32. Buttlar W. G., R. Roque, and B. Reid. “Automated Procedure for Generation of Creep Compliance Master Curve for Asphalt Mixtures.” *Transportation Research Record*, 1630 2836, 1998.

33. Jones, G. M., M. I. Darter, and G. Littlefield. “Thermal Expansion-Contraction of Asphaltic Concrete.” *Journal of the Association of Asphalt Paving Technologists*, 37, 1968, pp. 56–97.
34. Soules, T. F., R. F. Busbey, S. M. Rekhson, A. Markovsky, and M. A. Burke. “Finite-Element Calculation of Stresses in Glass Parts Undergoing Viscous Relaxation.” *Journal of the American Ceramic Society,* 70 (2), 1987, pp. 90–95.
35. Tran, N., R. West, B. Powell, and A. Kvasnak, “Evaluation of AASHTO Rut Test Procedure Using the Asphalt Pavement Analyzer.” *Journal of the Association of Asphalt Paving Technologists*, Minneapolis, MN, Vol 78, 2009, pp 1-24.

APPENDIX A PERFORMANCE GRADING OF RAP/RAS BLENDED WITH REJUVENATOR AT VARIOUS RATES

Sample ID: EAP RAP 0% Cyclogen

Test Method			**Test Results**	**Specification**
Rolling Thin Film (RTFO) Aged Binder, AASHTO T 240				
Rotational Viscosity @ 135°C, AASHTO T 316, PaS			5.61	≤ 3 PaS
Dynamic Shear Rheometer AASHTO T 315				
Test Temperature, °C	G*, kPa	Phase Angle δ, °	G* / sinδ, kPa	
94	3.87	79.0	3.95	≥ 2.20 kPa
100	1.97	81.7	1.99	
Pressure Aging Vessel (PAV) Aged Binder, AASHTO R28				
Dynamic Shear Rheometer AASHTO T 315				
Test Temperature, °C	G*, kPa	Phase Angle δ, °	G* sinδ, kPa	
34	7674	37.0	4619	≤ 5,000 kPa
31	10340	35.1	5954	
Bending Beam Rheometer (BBR) AASHTO T313				
Test Temperature, °C				
0	Stiffness, Mpa		101	≤ 300 Mpa
	m-value		0.295	≥ 0.300
-6	Stiffness, Mpa		185	
	m-value		0.259	
True Grade	99.1 – 9.2			
PG Grade	94 - 4			

1. DSR RTFO: T_{max}
   Temperature at which G*/sinδ = 2.20 kPa — 99.1
2. DSR PAV: T_{int}
   Temperature at which G*sinδ = 5,000 kPa — 33.1
3. BBR PAV: T_{min}
   Tempearautre at which S(t) = 300 Mpa — -24.2
   Temperature at which m = 0.300 — -9.2

Sample ID: **EAP RAP** **12% Cyclogen**

Test Method			**Test Results**	**Specification**
Rolling Thin Film (RTFO) Aged Binder, AASHTO T 240				
Rotational Viscosity @ 135°C, AASHTO T 316, PaS			1.65	≤ 3 PaS
Dynamic Shear Rheometer AASHTO T 315				
Test Temperature, °C	G*, kPa	Phase Angle δ, °	G* / sinδ, kPa	
82	2.63	80.9	2.66	≥ 2.20 kPa
88	1.32	83.3	1.33	
Pressure Aging Vessel (PAV) Aged Binder, AASHTO R28				
Dynamic Shear Rheometer AASHTO T 315				
Test Temperature, °C	G*, kPa	Phase Angle δ, °	G* sinδ, kPa	
25	5124	44.1	3565	≤ 5,000 kPa
22	7624	41.5	5056	
Bending Beam Rheometer (BBR) AASHTO T313				
Test Temperature, °C				
-12	Stiffness, Mpa		111	≤ 300 Mpa
	m-value		0.352	≥ 0.300
-18	Stiffness, Mpa		242	
	m-value		0.281	
True Grade	83.6 – 26.4			
PG Grade	82 - 22			

1. DSR RTFO: T_{max}
   Temperature at which G*/sinδ = 2.20 kPa — 83.6
2. DSR PAV: T_{int}
   Temperature at which G*sinδ = 5,000 kPa — 22.1
3. BBR PAV: T_{min}
   Tempearautre at which S(t) = 300 Mpa — -30.7
   Temperature at which m = 0.300 — -26.4

Sample ID: **EAP RAP** **20% Cyclogen**

Test Method			**Test Results**	**Specification**
Unaged Binder Tested as RTFO Binder				
Rotational Viscosity @ 135°C, AASHTO T 316, PaS			0.625	≤ 3 PaS
Dynamic Shear Rheometer AASHTO T 315				
Test Temperature, °C	G*, kPa	Phase Angle δ, °	G* / sinδ, kPa	
64	4.14	79.8	4.21	≥ 2.20 kPa
70	1.97	82.5	1.99	
Pressure Aging Vessel (PAV) Aged Binder, AASHTO R28				
Dynamic Shear Rheometer AASHTO T 315				
Test Temperature, °C	G*, kPa	Phase Angle δ, °	G* sinδ, kPa	
19	6022	46.6	4374	≤ 5,000 kPa
16	9354	43.7	6460	
Bending Beam Rheometer (BBR) AASHTO T313				
Test Temperature, °C				
-18	Stiffness, Mpa		191	≤ 300 Mpa
	m-value		0.344	≥ 0.300
-24	Stiffness, Mpa		442	
	m-value		0.261	
True Grade	0.0 -30.6			
PG Grade	64 - 28			

1. DSR RTFO: T_{max}
   Temperature at which G*/sinδ = 2.20 kPa — 69.2
2. DSR PAV: T_{int}
   Temperature at which G*sinδ = 5,000 kPa — 18.0
3. BBR PAV: T_{min}
   Tempearautre at which S(t) = 300 Mpa — -30.6
   Temperature at which m = 0.300 — -31.2

Sample ID: **RAS + 0% cyclogen**

Test Method			**Test Results**	**Specification**
Rolling Thin Film (RTFO) Aged Binder, AASHTO T 240				
Rotational Viscosity @ 135°C, AASHTO T 316, PaS				≤ 3 PaS
Dynamic Shear Rheometer AASHTO T 315				
Test Temperature, °C	G*, kPa	Phase Angle δ, °	G* / sinδ, kPa	
124	6.73	55.3	8.19	≥ 2.20 kPa
130	4.42	57.5	5.24	
Pressure Aging Vessel (PAV) Aged Binder, AASHTO R28				
Dynamic Shear Rheometer AASHTO T 315				
Test Temperature, °C	G*, kPa	Phase Angle δ, °	G* sinδ, kPa	
37	7833	31.1	4047	≤ 5,000 kPa
34	10120	29.9	5049	
Bending Beam Rheometer (BBR) AASHTO T313				
Test Temperature, °C				≤ 300 Mpa ≥ 0.300
6	Stiffness, Mpa			
	m-value			
0	Stiffness, Mpa		75	
	m-value		0.276	
True Grade	141.7 – 10.5			
PG Grade	136 - 4			

1. DSR RTFO: T_{max}
   Temperature at which G*/sinδ = 2.20 kPa — 141.7
2. DSR PAV: T_{int}
   Temperature at which G*sinδ = 5,000 kPa — 34.1
3. BBR PAV: T_{min}
   Tempearautre at which S(t) = 300 Mpa — -28.0
   Temperature at which m = 0.300 — -10.5

Sample ID: **RAS + 10% cyclogen**

Test Method			**Test Results**	**Specification**
Rolling Thin Film (RTFO) Aged Binder, AASHTO T 240				
Rotational Viscosity @ 135°C, AASHTO T 316, PaS				≤ 3 PaS
Dynamic Shear Rheometer AASHTO T 315				
Test Temperature, °C	G*, kPa	Phase Angle δ, °	G* / sinδ, kPa	
118	2.24	61.0	2.56	≥ 2.20 kPa
124	1.46	62.8	1.64	
Pressure Aging Vessel (PAV) Aged Binder, AASHTO R28				
Dynamic Shear Rheometer AASHTO T 315				
Test Temperature, °C	G*, kPa	Phase Angle δ, °	G* sinδ, kPa	
25	8232	34.0	4608	≤ 5,000 kPa
22	10970	32.7	5932	
Bending Beam Rheometer (BBR) AASHTO T313				
Test Temperature, °C				
-12	Stiffness, Mpa		124	≤ 300 Mpa
	m-value		0.304	≥ 0.300
-18	Stiffness, Mpa		242	
	m-value		0.272	
True Grade	120.1 – 22.8			
PG Grade	118 - 22			

1. DSR RTFO: T_{max}
   Temperature at which G*/sinδ = 2.20 kPa — 120.1
2. DSR PAV: T_{int}
   Temperature at which G*sinδ = 5,000 kPa — 24.0
3. BBR PAV: T_{min}
   Tempearautre at which S(t) = 300 Mpa — -30.9
   Temperature at which m = 0.300 — -22.8

Sample ID: **RAS + 20% cyclogen**

Test Method			**Test Results**	**Specification**
Unaged Binder Tested as RTFO Binder				
Rotational Viscosity @ 135°C, AASHTO T 316, PaS				≤ 3 PaS
Dynamic Shear Rheometer AASHTO T 315				
Test Temperature, °C	G*, kPa	Phase Angle δ, °	G* / sinδ, kPa	
94	2.51	63.1	2.81	≥ 2.20 kPa
100	1.54	65.4	1.69	
Pressure Aging Vessel (PAV) Aged Binder, AASHTO R28				
Dynamic Shear Rheometer AASHTO T 315				
Test Temperature, °C	G*, kPa	Phase Angle δ, °	G* sinδ, kPa	
19	4866	41.0	3192	≤ 5,000 kPa
16	6939	39.6	4422	
Bending Beam Rheometer (BBR) AASHTO T313				
Test Temperature, °C				
-12	Stiffness, Mpa		53	≤ 300 Mpa
	m-value		0.372	≥ 0.300
-18	Stiffness, Mpa		133	
	m-value		0.331	
True Grade	96.9 – 32.5			
PG Grade	94 - 28			

1. DSR RTFO: T_{max}
   Temperature at which G*/sinδ = 2.20 kPa — 96.9
2. DSR PAV: T_{int}
   Temperature at which G*sinδ = 5,000 kPa — 14.9
3. BBR PAV: T_{min}
   Tempearautre at which S(t) = 300 Mpa — -40.5
   Temperature at which m = 0.300 — -32.5

APPENDIX B PERFORMANCE GRADING OF VIRGIN AND BLENDED BINDERS

Sample ID: **Virgin Binder PG 67-22**

Test Method			**Test Results**	**Specification**
Original Binder				
Rotational Viscosity @ 135°C, AASHTO T 316, PaS			0.47	≤ 3 PaS
Dynamic Shear Rheometer AASHTO T 315				
Test Temperature, °C	G*, kPa	Phase Angle δ, °	G* / sinδ, kPa	
64	1.44	86.4	1.44	≥ 1.00 kPa
70	0.69	84.5	0.69	
Rolling Thin Film (RTFO) Aged Binder, AASHTO T 240				
Mass Change, %				≤ 1.00%
Dynamic Shear Rheometer AASHTO T 315				
Test Temperature, °C	G*, kPa	Phase Angle δ, °	G* / sinδ, kPa	
64	3.44	82.7	3.47	≥ 2.20 kPa
70	1.57	84.4	1.58	
Pressure Aging Vessel (PAV) Aged Binder, AASHTO R28				
Dynamic Shear Rheometer AASHTO T 315				
Test Temperature, °C	G*, kPa	Phase Angle δ, °	G* sinδ, kPa	
25	6373	43.3	4368	≤ 5,000 kPa
22	9631	40.4	6240	
Bending Beam Rheometer (BBR) AASHTO T313				
Test Temperature, °C				
-12	Stiffness, Mpa		201	≤ 300 Mpa
	m-value		0.312	≥ 0.300
-18	Stiffness, Mpa		378	
	m-value		0.253	
True Grade	67.0 -23.2			
PG Grade	64 - 22			

1. DSR Original: T_{max}
   Temperature at which G*/sinδ = 1.00 kPa — 67.0
2. DSR RTFO: T_{max}
   Temperature at which G*/sinδ = 2.20 kPa — 67.5
3. DSR PAV: T_{int}
   Temperature at which G*sinδ = 5,000 kPa — 23.9
4. BBR PAV: T_{min}
   Tempearautre at which S(t) = 300 Mpa — -25.4
   Temperature at which m = 0.300 — -23.2

Sample ID: **67-22 + 50% RAP Binder, No Cyclogen**

Test Method			**Test Results**	**Specification**
Original Binder				
Rotational Viscosity @ 135°C, AASHTO T 316, PaS				≤ 3 PaS
Dynamic Shear Rheometer AASHTO T 315				
Test Temperature, °C	G*, kPa	Phase Angle δ, °	G* / sinδ, kPa	
82	1.66	83.4	1.67	≥ 1.00 kPa
88	0.84	85.2	0.84	
Rolling Thin Film (RTFO) Aged Binder, AASHTO T 240				
Mass Change, %				≤ 1.00%
Dynamic Shear Rheometer AASHTO T 315				
Test Temperature, °C	G*, kPa	Phase Angle δ, °	G* / sinδ, kPa	
82	3.15	80	3.19	≥ 2.20 kPa
88	1.59	82.4	1.60	
Pressure Aging Vessel (PAV) Aged Binder, AASHTO R28				
Dynamic Shear Rheometer AASHTO T 315				
Test Temperature, °C	G*, kPa	Phase Angle δ, °	G* sinδ, kPa	
25	9887	36.4	5862	≤ 5,000 kPa
22	13960	34	7796	
Bending Beam Rheometer (BBR) AASHTO T313				
Test Temperature, oC				
-6	Stiffness, Mpa		132	≤ 300 Mpa
	m-value		0.319	≥ 0.300
-12	Stiffness, Mpa		254	
	m-value		0.267	
True Grade	85.2 -18.2			
PG Grade	82 - 16			

1. DSR Original: Tmax
   Temperature at which G*/sinδ = 1.00 kPa — 86.5
2. DSR RTFO:
Tmax
   Temperature at which G*/sinδ = 2.20 kPa — 85.2
3. DSR PAV: Tint
   Temperature at which G*sinδ = 5,000 kPa — 26.7
4. BBR PAV: Tmin
   Tempearautre at which S(t) = 300 Mpa — -24.3
   Temperature at which m = 0.300 — -18.2

Sample ID: 67-22 + 50% RAP Binder + 12% Cyclogen as Additive

Test Method			Test Results	Specification
Original Binder				
Rotational Viscosity @ 135°C, AASHTO T 316, PaS			0.833	≤ 3 PaS
Dynamic Shear Rheometer AASHTO T 315				
Test Temperature, °C	G*, kPa	Phase Angle δ, °	G* / sinδ, kPa	
76	1.62	83.9	1.63	≥ 1.00 kPa
82	0.80	85.6	0.80	
Rolling Thin Film (RTFO) Aged Binder, AASHTO T 240				
Mass Change, %			-0.539	≤ 1.00%
Dynamic Shear Rheometer AASHTO T 315				
Test Temperature, °C	G*, kPa	Phase Angle δ, °	G* / sinδ, kPa	
76	3.44	80.2	3.49	≥ 2.20 kPa
82	1.69	82.6	1.71	
Pressure Aging Vessel (PAV) Aged Binder, AASHTO R28				
Dynamic Shear Rheometer AASHTO T 315				
Test Temperature, °C	G*, kPa	Phase Angle δ, °	G* sinδ, kPa	
28	6059	42.3	4079	≤ 5,000 kPa
25	8862	39.7	5661	
Bending Beam Rheometer (BBR) AASHTO T313				
Test Temperature, °C				
-6	Stiffness, Mpa		100	≤ 300 Mpa
	m-value		0.34	≥ 0.300
-12	Stiffness, Mpa		193	
	m-value		0.294	
True Grade	79.9 – 21.2			
PG Grade	76 - 16			

1. DSR Original: T_{max}
   Temperature at which G*/sinδ = 1.00 kPa — 80.1
2. DSR RTFO: T_{max}
   Temperature at which G*/sinδ = 2.20 kPa — 79.9
3. DSR PAV: T_{int}
   Temperature at which G*sinδ = 5,000 kPa — 26.1
4. BBR PAV: T_{min}
   Tempearautre at which S(t) = 300 Mpa — -28.9
   Temperature at which m = 0.300 — -21.2

Sample ID: **67-22 + 20% RAP Binder + 5% RAS Binder, No Cyclogen**

Test Method			**Test Results**	**Specification**
Original Binder				
Rotational Viscosity @ 135°C, AASHTO T 316, PaS			0.988	≤ 3 PaS
Dynamic Shear Rheometer AASHTO T 315				
Test Temperature, °C	G*, kPa	Phase Angle δ, °	G* / sinδ, kPa	
82	1.27	82.3	1.28	≥ 1.00 kPa
88	0.68	83.9	0.68	
Rolling Thin Film (RTFO) Aged Binder, AASHTO T 240				
Mass Change, %			-0.325	≤ 1.00%
Dynamic Shear Rheometer AASHTO T 315				
Test Temperature, °C	G*, kPa	Phase Angle δ, °	G* / sinδ, kPa	
82	3.16	77.4	3.23	≥ 2.20 kPa
88	1.63	79.9	1.65	
Pressure Aging Vessel (PAV) Aged Binder, AASHTO R28				
Dynamic Shear Rheometer AASHTO T 315				
Test Temperature, °C	G*, kPa	Phase Angle δ, °	G* sinδ, kPa	
25	6666	36.9	4001	≤ 5,000 kPa
22	9400	34.7	5344	
Bending Beam Rheometer (BBR) AASHTO T313				
Test Temperature, oC				
-6	Stiffness, Mpa		122	≤ 300 Mpa
	m-value		0.32	≥ 0.300
-12	Stiffness, Mpa		231	
	m-value		0.285	
True Grade	84.3 -19.4			
PG Grade	82 - 16			

1. DSR Original: Tmax
   Temperature at which G*/sinδ = 1.00 kPa — 84.3
2. DSR RTFO: Tmax
   Temperature at which G*/sinδ = 2.20 kPa — 85.4
3. DSR PAV: Tint
   Temperature at which G*sinδ = 5,000 kPa — 22.7
4. BBR PAV: Tmin
   Tempearautre at which S(t) = 300 Mpa — -25.8
   Temperature at which m = 0.300 — -19.4

Sample ID: 67-22 + 20% RAP Binder + 5% RAS Binder+ 12% Cyclogen as Additive

Test Method			**Test Results**	**Specification**
Original Binder				
Rotational Viscosity @ 135°C, AASHTO T 316, PaS			0.988	≤ 3 PaS
Dynamic Shear Rheometer AASHTO T 315				
Test Temperature, °C	G*, kPa	Phase Angle δ, °	G* / sinδ, kPa	
88	1.02	66.8	1.11	≥ 1.00 kPa
94	0.70	63.1	0.78	
Rolling Thin Film (RTFO) Aged Binder, AASHTO T 240				
Mass Change, %			-0.325	≤ 1.00%
Dynamic Shear Rheometer AASHTO T 315				
Test Temperature, °C	G*, kPa	Phase Angle δ, °	G* / sinδ, kPa	
76	3.36	78.4	3.43	≥ 2.20 kPa
82	1.71	80.7	1.73	
Pressure Aging Vessel (PAV) Aged Binder, AASHTO R28				
Dynamic Shear Rheometer AASHTO T 315				
Test Temperature, °C	G*, kPa	Phase Angle δ, °	G* sinδ, kPa	
28	5399	42.5	3650	≤ 5,000 kPa
25	7901	40.11	5091	
Bending Beam Rheometer (BBR) AASHTO T313				
Test Temperature, °C				
-6	Stiffness, Mpa		90	≤ 300 Mpa
	m-value		0.349	≥ 0.300
-12	Stiffness, Mpa		193	
	m-value		0.294	
True Grade	79.9 – 21.3			
PG Grade	76 - 16			

1. DSR Original: T_{max}
   Temperature at which G*/sinδ = 1.00 kPa — 89.8
2. DSR RTFO: T_{max}
   Temperature at which G*/sinδ = 2.20 kPa — 79.9
3. DSR PAV: T_{int}
   Temperature at which G*sinδ = 5,000 kPa — 25.2
4. BBR PAV: T_{min}
   Tempearautre at which S(t) = 300 Mpa — -28.2
   Temperature at which m = 0.300 — -21.3

APPENDIX C OVERVIEW OF LINEAR AMPLITUDE SWEEP TEST

Background

The Linear Amplitude Sweep (LAS) test is an accelerated binder fatigue test that has been proposed to replace the current DSR intermediate temperature G*sinδ parameter. The current parameter is based on the assumption that the asphalt binders in pavements function in the linear-viscoelastic range and are therefore insensitive to strain levels. These assumptions have long been challenged, especially with the increased use of modified asphalts that have been shown to exhibit increased fatigue resistance and non-linear strain response. The LAS test was developed in response to the need for a fatigue test that could account for actual damage resistance as well as pavement structure and traffic loading. The LAS procedure uses cyclic loading with increasing load amplitude to accelerate damage. The end result is a prediction of binder fatigue life as a function of strain in the pavement.

The LAS test is run in the Dynamic Shear Rheometer (DSR) and consists of a frequency sweep at a strain level of 0.1% followed by a strain sweep test at a constant frequency of 10 Hz with linearly increasing strain amplitude (0.1 to 30%). It is performed on asphalt binder that has been aged in the Rolling Thin Film Oven (RTFO) using the 8 mm plates currently available for DSR intermediate temperature testing. The test temperature corresponds with either the tested intermediate temperature grade of the asphalt binder or the climatic intermediate temperature at a location where the asphalt binder is to be used.

Analysis of the LAS data is performed using viscoelastic continuum damage (VECD) theory which is based on Schapery's theory of work potential to model damage growth. Schapery's work potential theory is stated in the following form.

$$\frac{dD}{dt} = \left(\frac{\partial W}{\partial D}\right)^{\alpha} \tag{C1}$$

where:

D = Damage intensity
W = Work performed
α = Material constant related to the rate at which damage progresses (*1*)

Procedure

The LAS test is performed in two steps, both of which may be conducted using the same asphalt binder sample, and the total testing time is approximately 30 minutes. All testing for this study was performed at 32.1°C which corresponds to the local climate intermediate temperature.

Step 1

The LAS procedure begins with a DSR frequency sweep from 0.1 to 30 Hz. A low strain level of 0.1% is chosen so as not to induce damage into the sample. Data collected includes complex shear modulus (G*, Pa), and phase angle (δ, degrees). The data gathered in this step is used to determine the material constant, α. α is typically calculated as a function of the slope of a log-

log plot of relaxation modulus versus time. Because not all DSRs are capable of performing a stress relaxation test to determine this value, work done by Johnson and Bahia (*2*) showed that frequency sweep data could be converted to relaxation modulus. Further work by Hintz, et al. (*1*), simplified this process by demonstrating that this relationship could be estimated using the slope, m, of a log-log plot of storage modulus (G* cos(δ)) versus frequency (Figure 1). The resulting calculation is shown in equation 2.

$$\alpha = 1 + \frac{1}{m} \tag{2}$$

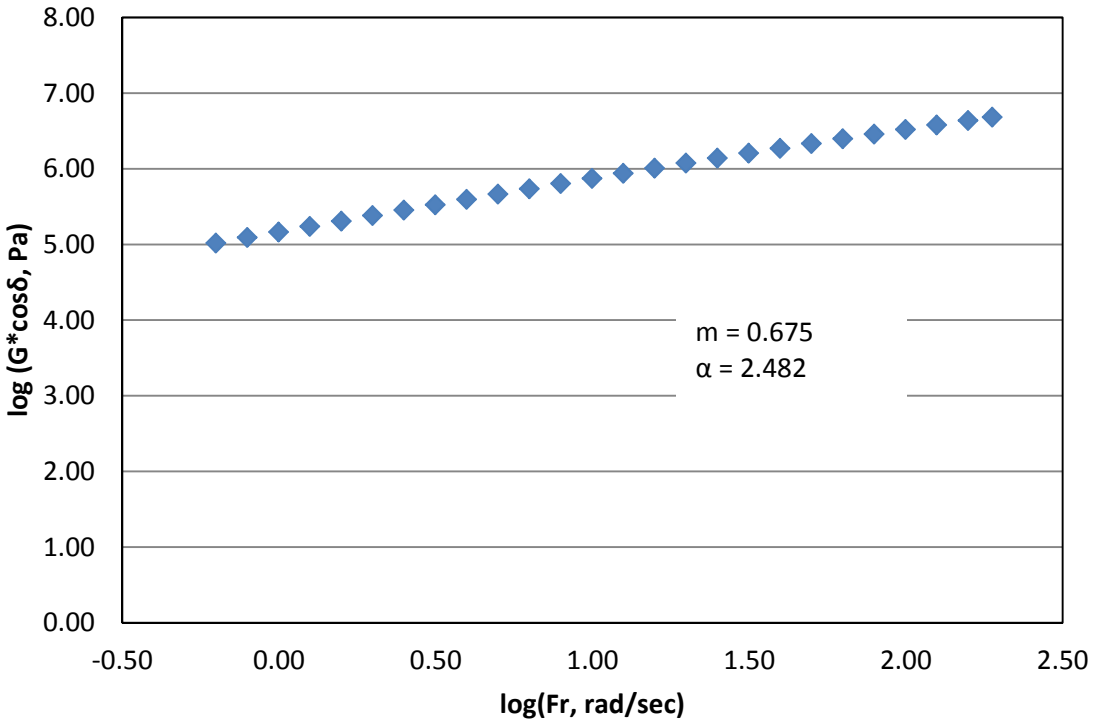

Figure 1 Calculation of α Parameter Using Frequency Sweep Results

Step 2

The next step in the LAS procedure is to perform a strain sweep on the asphalt binder sample. This step uses increasing load amplitudes to create damage in the sample. The strain sweep begins at 0.1% strain and increases linearly to 30% strain. At each strain level, multiple readings of G*, δ, and oscillatory stress are recorded. Accumulated damage levels in the specimen are calculated for each data point using equation 3.

$$D(t) \cong \sum_{i=1}^{N} [\pi I_D \gamma_0^2 (|G^*| sin\delta_{i-1} - |G^*| sin\delta_i)]^{\frac{\alpha}{1+\alpha}} (t_i - t_{i-1})^{\frac{1}{1+\alpha}} \tag{3}$$

where:

I_D = Average value of |G*| from the initial interval of 0.1% applied strain, MPa

γ_0 = Applied strain for a given data point, dimensionless
|G*| = Dynamic Shear Modulus, MPa
α = Value determined in Equation 2
t = Testing time, sec

Only damage levels above 100 are considered for the analysis, as damage levels below this value exhibit non-linear behavior. The data points calculated using equation 3 are used to determine the constants needed to form the relationship shown in equation 4.

$$|G^*|sin\delta = C_0 - C_1(D)^{C_2} \quad (4)$$

where:

C_0 = Average value of |G*|sinδ from the 0.1% strain interval
$Log(C_1)$ = Intercept of a line formed as log(C0-|G*|sinδ) versus log(D(t))
C_2 = Slope of a line formed as log(C0-|G*|sinδ) versus log(D(t))

Once the values of C_0, C_1, and C_2 have been determined, the damage corresponding to a 35% reduction in the undamaged |G*|sinδ (represented by C_0) is calculated using equation 5.

$$D_f = (0.35\frac{C_0}{C_1})^{\frac{1}{C_2}} \quad (5)$$

Finally, the binder fatigue performance parameter (N_f) can be calculated using equation 6. N_f can be adjusted to account for differences in pavement structure by changing γ_{max}. Higher strain values may correspond to thinner pavements or heavier traffic loading while lower strain values may correspond to thicker pavements or lighter traffic loads (*3*).

$$N_f = A(\gamma_{max})^B \quad (6)$$

where:

γ_{max} = Applied binder strain for a given pavement structure, dimensionless
B = -2α

$$A = \frac{f(D_f)^k}{k\left(\pi\frac{I_D}{|G^*|}C_1C_2\right)^\alpha}|G^*|^{-\alpha}$$

where:

f = loading frequency (10Hz)
k = $1 + (1-C_2)\alpha$
|G*| = average value of G* from the 0.1% applied strain interval, MPa.

An example of the data gathered in step 2 is shown in Figures 2 and 3.

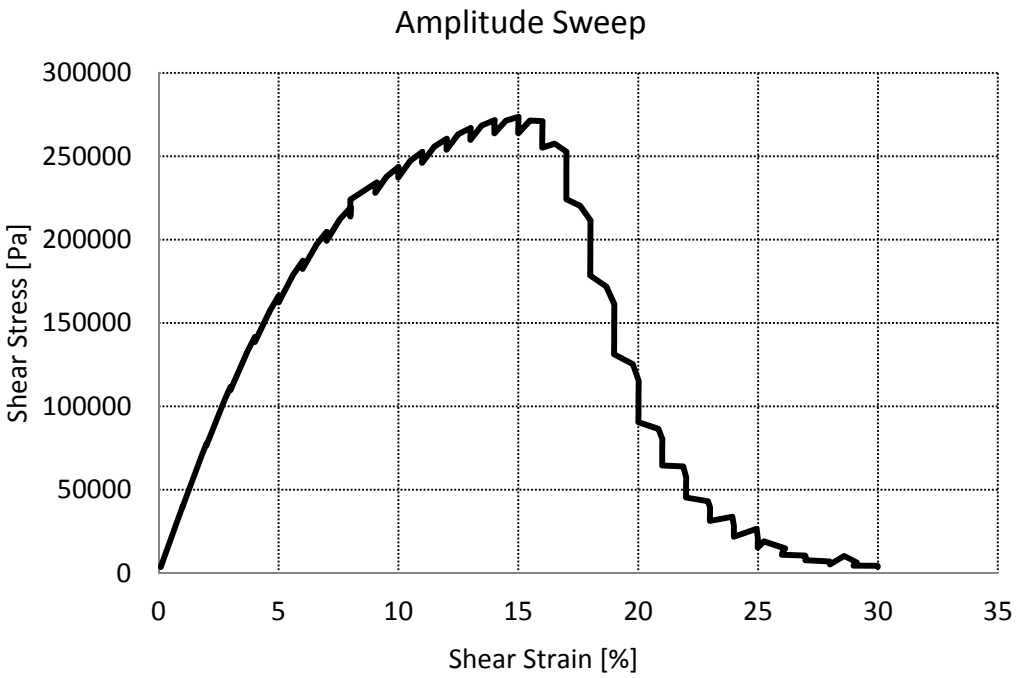

Figure 2 Plot of Shear Stress versus Shear Strain

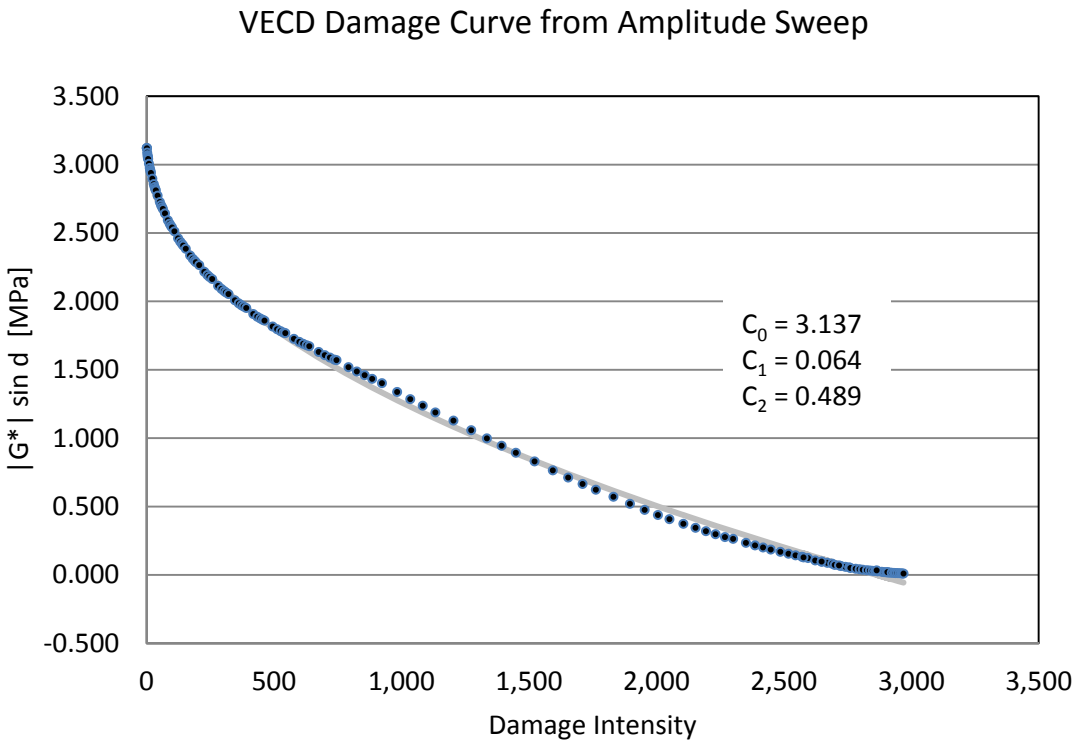

Figure 3 Damage Intensity Plot

Using the value of α found in Step 1 and the C parameters calculated in Step 2, binder fatigue parameters (N_f) are determined for two strain levels--2.5% and 5%. The higher strain level results in a shorter fatigue life.

References

1. Hintz, C., R. Velasquez, C. Johnson, H. Bahia, "Modification and Validation of the Linear Amplitude Sweep Test for Binder Fatigue Specification," Submitted for publication and presentation at the Transportation Research Board Annual Meeting, Washington, D.C., January 2011.
2. Johnson, C.M. and H.U. Bahia, "Evaluation of an Accelerated Procedure for Fatigue Characterization of Asphalt Binders," Submitted for publication in Road Materials and Pavement Design, 2010.
3. Standard Method of Test for Estimating Fatigue Resistance of Asphalt Binders Using the Linear Amplitude Sweep, Draft Test Method, 2009.

APPENDIX D RESULTS OF TSR TEST

%RAP	%RAS	Additive	Height (in.)	Diameter (in.)	Voids (%)	F/T Cyc.	Sat. (%)	Failure (lb)	Flow (0.01 in)	Strength (psi)
0	0	None	3.670	5.897	6.8	1	73.3	4200	17.0	123.5
0	0	None	3.665	5.900	7.1	1	78.0	3900	19.0	114.8
0	0	None	3.669	5.900	6.8	1	77.8	4200	17.0	123.5
0	0	None	3.669	5.895	6.8	0	0.0	4500	15.0	132.5
0	0	None	3.665	5.902	6.8	0	0.0	4400	16.0	129.5
0	0	None	3.727	5.898	6.7	0	0.0	4475	15.0	129.6
20	5	None	3.732	5.917	6.9	1	71.2	5300	7.0	152.8
20	5	None	3.733	5.909	6.6	1	70.6	5450	17.0	157.3
20	5	None	3.738	5.912	6.9	1	76.4	5400	15.5	155.6
20	5	None	3.740	5.924	7.1	0	0.0	5625	16.0	161.6
20	5	None	3.728	5.915	6.7	0	0.0	6200	15.0	179.0
20	5	None	3.734	5.915	6.7	0	0.0	6000	15.5	172.9
20	5	Cyclogen	3.724	5.933	7.3	1	72.4	4475	18.5	128.9
20	5	Cyclogen	3.726	5.933	7.5	1	70.5	4300	19.0	123.8
20	5	Cyclogen	3.730	5.931	6.9	1	71.6	4825	19.0	138.8
20	5	Cyclogen	3.721	5.932	7.3	0	0.0	4700	18.5	135.6
20	5	Cyclogen	3.726	5.924	6.9	0	0.0	5150	17.0	148.5
20	5	Cyclogen	3.741	5.929	7.4	0	0.0	4950	18.0	142.1
50	0	None	3.740	5.900	7.0	1	70.9	6100	14.0	176.0
50	0	None	3.740	5.900	7.1	1	73.9	5500	18.0	158.7
50	0	None	3.740	5.900	7.3	1	72.7	5850	14.0	168.8
50	0	None	3.740	5.900	7.1	0	0.0	7400	n/a	213.5
50	0	None	3.740	5.900	7.1	0	0.0	7650	12.5	220.7
50	0	None	3.740	5.900	7.2	0	0.0	6850	17.5	197.6
50	0	Cyclogen	3.715	5.914	6.5	1	74.0	5000	16.0	144.9
50	0	Cyclogen	3.715	5.927	7.3	1	79.1	4300	16.0	124.3
50	0	Cyclogen	3.714	5.923	7.2	1	75.0	4500	16.0	130.2
50	0	Cyclogen	3.714	5.918	7.1	0	0.0	5150	16.0	149.2
50	0	Cyclogen	3.714	5.918	7.0	0	0.0	5250	16.0	152.1
50	0	Cyclogen	3.719	5.926	7.5	0	0.0	5550	17.5	160.3

APPENDIX E RESULTS OF E* TEST

%RAP	%RAS	Additive	Aging	Voids (%)	Temp (Deg C)	Freq (Hz)	Test Date	Phase (deg)	E* (ksi)
0	0	None	STA	6.9	4	10	8/5/2011	0.6	1846.0
0	0	None	STA	6.9	4	1	8/5/2011	0.8	1335.4
0	0	None	STA	6.9	4	0.1	8/5/2011	0.9	895.9
0	0	None	STA	6.9	20	10	8/8/2011	0.4	812.4
0	0	None	STA	6.9	20	1	8/8/2011	0.4	463.0
0	0	None	STA	6.9	20	0.1	8/8/2011	0.4	240.5
0	0	None	STA	6.9	40	10	8/8/2011	0.3	293.8
0	0	None	STA	6.9	40	1	8/8/2011	0.4	130.7
0	0	None	STA	6.9	40	0.1	8/8/2011	0.8	57.6
0	0	None	STA	6.9	40	0.01	8/8/2011	2	26.4
0	0	None	STA	7	4	10	8/5/2011	0.4	1994.8
0	0	None	STA	7	4	1	8/5/2011	0.4	1457.6
0	0	None	STA	7	4	0.1	8/5/2011	0.5	982.6
0	0	None	STA	7	20	10	8/8/2011	0.2	830.2
0	0	None	STA	7	20	1	8/8/2011	0.3	469.3
0	0	None	STA	7	20	0.1	8/8/2011	0.2	241.6
0	0	None	STA	7	40	10	8/8/2011	0.2	241.2
0	0	None	STA	7	40	1	8/8/2011	0.4	104.2
0	0	None	STA	7	40	0.1	8/8/2011	0.8	46.8
0	0	None	STA	7	40	0.01	8/8/2011	2	24.7
0	0	None	STA	7.1	4	10	8/5/2011	0.4	1852.6
0	0	None	STA	7.1	4	1	8/5/2011	0.6	1342.9
0	0	None	STA	7.1	4	0.1	8/5/2011	0.7	897.2
0	0	None	STA	7.1	20	10	8/8/2011	0.4	772.8
0	0	None	STA	7.1	20	1	8/8/2011	0.1	430.9
0	0	None	STA	7.1	20	0.1	8/8/2011	0	217.3
0	0	None	STA	7.1	40	10	8/9/2011	0.2	216.7
0	0	None	STA	7.1	40	1	8/9/2011	1.1	90.6
0	0	None	STA	7.1	40	0.1	8/9/2011	1.7	40.2
0	0	None	STA	7.1	40	0.01	8/9/2011	2	21.0
0	0	None	STA	6.9	4	10	9/7/2011	0.6	1924.7
0	0	None	STA	6.9	4	1	9/7/2011	0.6	1440.9
0	0	None	STA	6.9	4	0.1	9/7/2011	0.8	1002.2
0	0	None	STA	6.9	20	10	9/8/2011	0.8	825.0
0	0	None	STA	6.9	20	1	9/8/2011	0.7	477.5
0	0	None	STA	6.9	20	0.1	9/8/2011	0.6	254.5
0	0	None	STA	6.9	40	10	9/8/2011	0.9	244.0
0	0	None	STA	6.9	40	1	9/8/2011	1.1	107.0

%RAP	%RAS	Additive	Aging	Voids (%)	Temp (Deg C)	Freq (Hz)	Test Date	Phase (deg)	E* (ksi)
0	0	None	STA	6.9	40	0.1	9/8/2011	1.7	49.2
0	0	None	STA	6.9	40	0.01	9/8/2011	2.2	26.4
0	0	None	STA	7	4	10	9/7/2011	0.6	2112.2
0	0	None	STA	7	4	1	9/7/2011	0.6	1546.5
0	0	None	STA	7	4	0.1	9/7/2011	0.7	1068.6
0	0	None	STA	7	20	10	9/8/2011	0.5	867.3
0	0	None	STA	7	20	1	9/8/2011	0.4	497.5
0	0	None	STA	7	20	0.1	9/8/2011	0.5	265.1
0	0	None	STA	7	40	10	9/9/2011	1.1	304.6
0	0	None	STA	7	40	1	9/9/2011	1.5	140.0
0	0	None	STA	7	40	0.1	9/9/2011	1.8	60.8
0	0	None	STA	7	40	0.01	9/9/2011	2.4	25.9
0	0	None	STA	7.1	4	10	9/7/2011	0.3	1890.1
0	0	None	STA	7.1	4	1	9/7/2011	0.4	1393.4
0	0	None	STA	7.1	4	0.1	9/7/2011	0.4	958.7
0	0	None	STA	7.1	20	10	9/8/2011	0.8	793.8
0	0	None	STA	7.1	20	1	9/8/2011	0.7	458.0
0	0	None	STA	7.1	20	0.1	9/8/2011	0.5	240.6
0	0	None	STA	7.1	40	10	9/9/2011	1.3	235.0
0	0	None	STA	7.1	40	1	9/9/2011	1.6	101.3
0	0	None	STA	7.1	40	0.1	9/9/2011	2.6	44.9
0	0	None	STA	7.1	40	0.01	9/9/2011	3.4	22.3
0	0	None	LTA	7.3	4	10	9/1/2011	0.6	1906.1
0	0	None	LTA	7.3	4	1	9/1/2011	0.4	1417.5
0	0	None	LTA	7.3	4	0.1	9/1/2011	0.2	985.4
0	0	None	LTA	7.3	20	10	9/6/2011	0.8	859.1
0	0	None	LTA	7.3	20	1	9/6/2011	0.8	501.0
0	0	None	LTA	7.3	20	0.1	9/6/2011	0.8	265.6
0	0	None	LTA	7.3	40	10	10/4/2011	0.6	265.1
0	0	None	LTA	7.3	40	1	10/4/2011	0.9	116.9
0	0	None	LTA	7.3	40	0.1	10/4/2011	1.5	50.8
0	0	None	LTA	7.3	40	0.01	10/4/2011	2.4	23.5
0	0	None	LTA	7.4	4	10	9/1/2011	1.3	2146.4
0	0	None	LTA	7.4	4	1	9/1/2011	1.2	1578.9
0	0	None	LTA	7.4	4	0.1	9/1/2011	1.3	1080.5
0	0	None	LTA	7.4	20	10	9/6/2011	0.6	939.1
0	0	None	LTA	7.4	20	1	9/6/2011	0.7	546.2
0	0	None	LTA	7.4	20	0.1	9/6/2011	0.7	289.9
0	0	None	LTA	7.4	40	10	9/15/2011	1	271.8
0	0	None	LTA	7.4	40	1	9/15/2011	1.2	119.8

%RAP	%RAS	Additive	Aging	Voids (%)	Temp (Deg C)	Freq (Hz)	Test Date	Phase (deg)	E* (ksi)
0	0	None	LTA	7.4	40	0.1	9/15/2011	1	53.3
0	0	None	LTA	7.4	40	0.01	9/15/2011	1.4	26.7
0	0	None	LTA	7.5	4	10	9/1/2011	1.8	2016.5
0	0	None	LTA	7.5	4	1	9/1/2011	1.6	1507.8
0	0	None	LTA	7.5	4	0.1	9/1/2011	1.5	1052.0
0	0	None	LTA	7.5	20	10	9/6/2011	0.7	882.7
0	0	None	LTA	7.5	20	1	9/6/2011	0.9	523.6
0	0	None	LTA	7.5	20	0.1	9/6/2011	1	283.5
0	0	None	LTA	7.5	40	10	9/15/2011	1.1	250.9
0	0	None	LTA	7.5	40	1	9/15/2011	1.3	110.3
0	0	None	LTA	7.5	40	0.1	9/15/2011	1.5	49.1
0	0	None	LTA	7.5	40	0.01	9/15/2011	1.7	24.9
20	5	None	STA	7.2	4	10	8/26/2011	0.1	1856.9
20	5	None	STA	7.2	4	1	8/26/2011	0.3	1421.9
20	5	None	STA	7.2	4	0.1	8/26/2011	0.1	1038.9
20	5	None	STA	7.2	20	10	9/6/2011	0.5	939.3
20	5	None	STA	7.2	20	1	9/6/2011	0.6	603.4
20	5	None	STA	7.2	20	0.1	9/6/2011	0.5	359.3
20	5	None	STA	7.2	45	10	9/12/2011	1	211.0
20	5	None	STA	7.2	45	1	9/12/2011	1.2	99.3
20	5	None	STA	7.2	45	0.1	9/12/2011	1.7	48.4
20	5	None	STA	7.2	45	0.01	9/12/2011	2.4	24.9
20	5	None	STA	7.1	4	10	8/26/2011	0.3	1948.4
20	5	None	STA	7.1	4	1	8/26/2011	0.5	1502.7
20	5	None	STA	7.1	4	0.1	8/26/2011	0.8	1097.2
20	5	None	STA	7.1	20	10	9/6/2011	0.5	982.1
20	5	None	STA	7.1	20	1	9/6/2011	0.5	633.8
20	5	None	STA	7.1	20	0.1	9/6/2011	0.4	377.0
20	5	None	STA	7.1	45	10	9/13/2011	0.7	220.5
20	5	None	STA	7.1	45	1	9/13/2011	0.6	104.5
20	5	None	STA	7.1	45	0.1	9/13/2011	1.1	51.4
20	5	None	STA	7.1	45	0.01	9/13/2011	1.7	27.3
20	5	None	STA	7.2	4	10	9/6/2011	0.8	1983.7
20	5	None	STA	7.2	4	1	9/6/2011	0.4	1531.5
20	5	None	STA	7.2	4	0.1	9/6/2011	0.2	1126.4
20	5	None	STA	7.2	20	10	9/6/2011	0.4	980.3
20	5	None	STA	7.2	20	1	9/6/2011	0.6	626.7
20	5	None	STA	7.2	20	0.1	9/6/2011	0.7	370.4
20	5	None	STA	7.2	45	10	9/13/2011	1	230.2
20	5	None	STA	7.2	45	1	9/13/2011	1.4	109.4

%RAP	%RAS	Additive	Aging	Voids (%)	Temp (Deg C)	Freq (Hz)	Test Date	Phase (deg)	E* (ksi)
20	5	None	STA	7.2	45	0.1	9/13/2011	1.7	53.3
20	5	None	STA	7.2	45	0.01	9/13/2011	2	27.7
20	5	None	STA	7.2	4	10	9/30/2011	0.1	1983.7
20	5	None	STA	7.2	4	1	9/30/2011	0.2	1542.5
20	5	None	STA	7.2	4	0.1	9/30/2011	0.3	1145.7
20	5	None	STA	7.2	20	10	9/30/2011	0.4	998.1
20	5	None	STA	7.2	20	1	9/30/2011	0.5	651.8
20	5	None	STA	7.2	20	0.1	9/30/2011	0.4	394.9
20	5	None	STA	7.2	45	10	10/3/2011	0.4	240.3
20	5	None	STA	7.2	45	1	10/3/2011	0.5	116.1
20	5	None	STA	7.2	45	0.1	10/3/2011	1.2	56.3
20	5	None	STA	7.2	45	0.01	10/3/2011	2	28.5
20	5	None	STA	7.1	4	10	9/30/2011	0.2	2060.6
20	5	None	STA	7.1	4	1	9/30/2011	0.2	1608.6
20	5	None	STA	7.1	4	0.1	9/30/2011	0.2	1194.2
20	5	None	STA	7.1	20	10	9/30/2011	0.2	1011.5
20	5	None	STA	7.1	20	1	9/30/2011	0.2	648.0
20	5	None	STA	7.1	20	0.1	9/30/2011	0	389.9
20	5	None	STA	7.1	45	10	10/3/2011	0.7	232.1
20	5	None	STA	7.1	45	1	10/3/2011	0.8	112.3
20	5	None	STA	7.1	45	0.1	10/3/2011	1.1	55.1
20	5	None	STA	7.1	45	0.01	10/3/2011	1.9	29.5
20	5	None	STA	7.2	4	10	9/30/2011	0.1	2089.0
20	5	None	STA	7.2	4	1	9/30/2011	0.3	1632.0
20	5	None	STA	7.2	4	0.1	9/30/2011	0.2	1216.6
20	5	None	STA	7.2	20	10	9/30/2011	0.3	1027.3
20	5	None	STA	7.2	20	1	9/30/2011	0.4	666.2
20	5	None	STA	7.2	20	0.1	9/30/2011	0.2	404.4
20	5	None	STA	7.2	45	10	10/3/2011	0.7	245.7
20	5	None	STA	7.2	45	1	10/3/2011	1.2	118.6
20	5	None	STA	7.2	45	0.1	10/3/2011	1.6	58.3
20	5	None	STA	7.2	45	0.01	10/3/2011	2.1	31.6
20	5	None	LTA	7.2	4	10	9/16/2011	0.6	1941.6
20	5	None	LTA	7.2	4	1	9/16/2011	0.8	1565.7
20	5	None	LTA	7.2	4	0.1	9/16/2011	0.9	1216.9
20	5	None	LTA	7.2	20	10	9/19/2011	0.7	981.2
20	5	None	LTA	7.2	20	1	9/19/2011	0.8	662.7
20	5	None	LTA	7.2	20	0.1	9/19/2011	0.7	421.0
20	5	None	LTA	7.2	45	10	9/20/2011	0.5	266.9
20	5	None	LTA	7.2	45	1	9/20/2011	0.5	135.5

%RAP	%RAS	Additive	Aging	Voids (%)	Temp (Deg C)	Freq (Hz)	Test Date	Phase (deg)	E* (ksi)
20	5	None	LTA	7.2	45	0.1	9/20/2011	0.8	66.4
20	5	None	LTA	7.2	45	0.01	9/20/2011	1.2	34.1
20	5	None	LTA	7.3	4	10	9/16/2011	0.4	2145.1
20	5	None	LTA	7.3	4	1	9/16/2011	0.8	1705.1
20	5	None	LTA	7.3	4	0.1	9/16/2011	0.8	1293.4
20	5	None	LTA	7.3	20	10	9/19/2011	0.7	1016.3
20	5	None	LTA	7.3	20	1	9/19/2011	0.9	662.5
20	5	None	LTA	7.3	20	0.1	9/19/2011	0.9	409.7
20	5	None	LTA	7.3	45	10	9/20/2011	1.6	259.5
20	5	None	LTA	7.3	45	1	9/20/2011	1.5	130.7
20	5	None	LTA	7.3	45	0.1	9/20/2011	1.5	65.6
20	5	None	LTA	7.3	45	0.01	9/20/2011	2.1	35.3
20	5	None	LTA	7.4	4	10	9/6/2011	0.7	2114.8
20	5	None	LTA	7.4	4	1	9/6/2011	0.8	1673.6
20	5	None	LTA	7.4	4	0.1	9/6/2011	0.7	1261.7
20	5	None	LTA	7.4	20	10	9/19/2011	0.6	983.8
20	5	None	LTA	7.4	20	1	9/19/2011	0.6	633.1
20	5	None	LTA	7.4	20	0.1	9/19/2011	0.5	383.8
20	5	None	LTA	7.4	45	10	10/4/2011	0.9	281.1
20	5	None	LTA	7.4	45	1	10/4/2011	0.9	139.9
20	5	None	LTA	7.4	45	0.1	10/4/2011	1.1	68.3
20	5	None	LTA	7.4	45	0.01	10/4/2011	1.7	32.1
20	5	Cyclogen	STA	7.2	4	10	9/26/2011	0.2	2006.3
20	5	Cyclogen	STA	7.2	4	1	9/26/2011	0.4	1460.5
20	5	Cyclogen	STA	7.2	4	0.1	9/26/2011	0.4	994.4
20	5	Cyclogen	STA	7.2	20	10	9/26/2011	0.4	851.4
20	5	Cyclogen	STA	7.2	20	1	9/26/2011	0.6	486.7
20	5	Cyclogen	STA	7.2	20	0.1	9/26/2011	0.5	256.9
20	5	Cyclogen	STA	7.2	45	10	9/27/2011	0.4	184.5
20	5	Cyclogen	STA	7.2	45	1	9/27/2011	1.4	81.2
20	5	Cyclogen	STA	7.2	45	0.1	9/27/2011	2.2	38.6
20	5	Cyclogen	STA	7.2	45	0.01	9/27/2011	3.4	22.5
20	5	Cyclogen	STA	7.1	4	10	9/26/2011	0.1	1952.4
20	5	Cyclogen	STA	7.1	4	1	9/26/2011	0.2	1452.0
20	5	Cyclogen	STA	7.1	4	0.1	9/26/2011	0.2	1009.0
20	5	Cyclogen	STA	7.1	20	10	9/26/2011	0.4	857.6
20	5	Cyclogen	STA	7.1	20	1	9/26/2011	0.3	499.5
20	5	Cyclogen	STA	7.1	20	0.1	9/26/2011	0.4	267.4
20	5	Cyclogen	STA	7.1	45	10	9/27/2011	0.4	176.5
20	5	Cyclogen	STA	7.1	45	1	9/27/2011	1.4	79.0

%RAP	%RAS	Additive	Aging	Voids (%)	Temp (Deg C)	Freq (Hz)	Test Date	Phase (deg)	E* (ksi)
20	5	Cyclogen	STA	7.1	45	0.1	9/27/2011	1.8	39.8
20	5	Cyclogen	STA	7.1	45	0.01	9/27/2011	1.5	25.5
20	5	Cyclogen	STA	7	4	10	9/26/2011	0.3	2109.9
20	5	Cyclogen	STA	7	4	1	9/26/2011	0.3	1553.2
20	5	Cyclogen	STA	7	4	0.1	9/26/2011	0.1	1066.2
20	5	Cyclogen	STA	7	20	10	9/26/2011	0.4	859.5
20	5	Cyclogen	STA	7	20	1	9/26/2011	0.5	492.8
20	5	Cyclogen	STA	7	20	0.1	9/26/2011	0.1	264.3
20	5	Cyclogen	STA	7	45	10	9/27/2011	0.5	179.1
20	5	Cyclogen	STA	7	45	1	9/27/2011	0.9	79.1
20	5	Cyclogen	STA	7	45	0.1	9/27/2011	1.2	39.2
20	5	Cyclogen	STA	7	45	0.01	9/27/2011	1.1	24.9
20	5	Cyclogen	LTA	6.9	4	10	10/7/2011	0.5	1927.6
20	5	Cyclogen	LTA	6.9	4	1	10/7/2011	0.7	1549.4
20	5	Cyclogen	LTA	6.9	4	0.1	10/7/2011	0.6	1183.2
20	5	Cyclogen	LTA	6.9	20	10	10/7/2011	0.7	894.4
20	5	Cyclogen	LTA	6.9	20	1	10/7/2011	0.8	569.1
20	5	Cyclogen	LTA	6.9	20	0.1	10/7/2011	0.6	337.6
20	5	Cyclogen	LTA	6.9	45	10	10/10/2011	0.5	228.4
20	5	Cyclogen	LTA	6.9	45	1	10/10/2011	0.7	105.7
20	5	Cyclogen	LTA	6.9	45	0.1	10/10/2011	1.1	51.5
20	5	Cyclogen	LTA	6.9	45	0.01	10/10/2011	0.9	27.4
20	5	Cyclogen	LTA	7.3	4	10	10/7/2011	0.4	2091.0
20	5	Cyclogen	LTA	7.3	4	1	10/7/2011	0.7	1634.9
20	5	Cyclogen	LTA	7.3	4	0.1	10/7/2011	0.6	1219.0
20	5	Cyclogen	LTA	7.3	20	10	10/7/2011	0.7	988.1
20	5	Cyclogen	LTA	7.3	20	1	10/7/2011	0.6	628.6
20	5	Cyclogen	LTA	7.3	20	0.1	10/7/2011	0.3	371.4
20	5	Cyclogen	LTA	7.3	45	10	10/10/2011	0.9	254.1
20	5	Cyclogen	LTA	7.3	45	1	10/10/2011	1	121.8
20	5	Cyclogen	LTA	7.3	45	0.1	10/10/2011	1.4	57.8
20	5	Cyclogen	LTA	7.3	45	0.01	10/10/2011	2	28.5
20	5	Cyclogen	LTA	6.7	4	10	10/11/2011	0.1	2189.2
20	5	Cyclogen	LTA	6.7	4	1	10/11/2011	0.1	1718.7
20	5	Cyclogen	LTA	6.7	4	0.1	10/11/2011	0.1	1283.3
20	5	Cyclogen	LTA	6.7	20	10	10/7/2011	0.8	1064.0
20	5	Cyclogen	LTA	6.7	20	1	10/7/2011	1.1	688.1
20	5	Cyclogen	LTA	6.7	20	0.1	10/7/2011	1.1	411.6
20	5	Cyclogen	LTA	6.7	45	10	10/10/2011	0.8	245.1
20	5	Cyclogen	LTA	6.7	45	1	10/10/2011	0.8	116.2

%RAP	%RAS	Additive	Aging	Voids (%)	Temp (Deg C)	Freq (Hz)	Test Date	Phase (deg)	E* (ksi)
20	5	Cyclogen	LTA	6.7	45	0.1	10/10/2011	1	56.2
20	5	Cyclogen	LTA	6.7	45	0.01	10/10/2011	1.5	29.1
50	0	None	STA	7	4	10	8/9/2011	1.1	2277.4
50	0	None	STA	7	4	1	8/9/2011	1.2	1822.0
50	0	None	STA	7	4	0.1	8/9/2011	1.1	1385.8
50	0	None	STA	7	20	10	8/10/2011	0.4	1122.3
50	0	None	STA	7	20	1	8/10/2011	0.3	736.4
50	0	None	STA	7	20	0.1	8/10/2011	0.2	439.3
50	0	None	STA	7	45	10	8/10/2011	0.4	309.4
50	0	None	STA	7	45	1	8/10/2011	1.1	145.3
50	0	None	STA	7	45	0.1	8/10/2011	1.8	66.3
50	0	None	STA	7	45	0.01	8/10/2011	2.2	30.5
50	0	None	STA	7	4	10	8/15/2011	0.7	2048.9
50	0	None	STA	7	4	1	8/15/2011	1	1618.0
50	0	None	STA	7	4	0.1	8/15/2011	1.1	1213.1
50	0	None	STA	7	20	10	8/16/2011	0.8	1089.7
50	0	None	STA	7	20	1	8/16/2011	0.5	713.7
50	0	None	STA	7	20	0.1	8/16/2011	0.1	430.0
50	0	None	STA	7	45	10	8/16/2011	0.2	265.9
50	0	None	STA	7	45	1	8/16/2011	0.7	123.6
50	0	None	STA	7	45	0.1	8/16/2011	1.2	56.4
50	0	None	STA	7	45	0.01	8/16/2011	1.3	27.5
50	0	None	STA	7	4	10	8/9/2011	1.1	2268.2
50	0	None	STA	7	4	1	8/9/2011	0.7	1797.0
50	0	None	STA	7	4	0.1	8/9/2011	1	1351.2
50	0	None	STA	7	20	10	8/10/2011	0.4	1045.0
50	0	None	STA	7	20	1	8/10/2011	0.5	667.9
50	0	None	STA	7	20	0.1	8/10/2011	0.3	393.1
50	0	None	STA	7	45	10	8/11/2011	0.3	300.4
50	0	None	STA	7	45	1	8/11/2011	0.6	143.8
50	0	None	STA	7	45	0.1	8/11/2011	1	65.9
50	0	None	STA	7	45	0.01	8/11/2011	1.7	29.5
50	0	None	STA	7	4	10	9/7/2011	0.2	2073.7
50	0	None	STA	7	4	1	9/7/2011	0.2	1667.4
50	0	None	STA	7	4	0.1	9/7/2011	0.2	1288.1
50	0	None	STA	7	20	10	9/8/2011	0.4	1089.1
50	0	None	STA	7	20	1	9/8/2011	0.3	736.8
50	0	None	STA	7	20	0.1	9/8/2011	0.4	459.9
50	0	None	STA	7	45	10	9/12/2011	1.1	299.8
50	0	None	STA	7	45	1	9/12/2011	1.5	145.2

%RAP	%RAS	Additive	Aging	Voids (%)	Temp (Deg C)	Freq (Hz)	Test Date	Phase (deg)	E* (ksi)
50	0	None	STA	7	45	0.1	9/12/2011	1.9	67.0
50	0	None	STA	7	45	0.01	9/12/2011	2.3	31.8
50	0	None	STA	7	4	10	9/7/2011	0.4	2030.2
50	0	None	STA	7	4	1	9/7/2011	0.4	1627.2
50	0	None	STA	7	4	0.1	9/7/2011	0.5	1244.3
50	0	None	STA	7	20	10	9/8/2011	0.4	1069.2
50	0	None	STA	7	20	1	9/8/2011	0.3	715.8
50	0	None	STA	7	20	0.1	9/8/2011	0.1	441.8
50	0	None	STA	7	45	10	9/12/2011	0.9	272.5
50	0	None	STA	7	45	1	9/12/2011	1.1	129.3
50	0	None	STA	7	45	0.1	9/12/2011	1.1	60.1
50	0	None	STA	7	45	0.01	9/12/2011	1.4	28.5
50	0	None	STA	7	4	10	9/7/2011	0.3	2300.0
50	0	None	STA	7	4	1	9/7/2011	0.2	1808.9
50	0	None	STA	7	4	0.1	9/7/2011	0.2	1354.7
50	0	None	STA	7	20	10	9/8/2011	0.4	1156.4
50	0	None	STA	7	20	1	9/8/2011	0.3	754.8
50	0	None	STA	7	20	0.1	9/8/2011	0.2	454.5
50	0	None	STA	7	45	10	9/12/2011	0.8	272.7
50	0	None	STA	7	45	1	9/12/2011	0.7	128.6
50	0	None	STA	7	45	0.1	9/12/2011	0.7	58.6
50	0	None	STA	7	45	0.01	9/12/2011	1.5	27.7
50	0	None	LTA	7	4	10	9/1/2011	0.9	2189.1
50	0	None	LTA	7	4	1	9/1/2011	0.8	1795.9
50	0	None	LTA	7	4	0.1	9/1/2011	0.7	1419.8
50	0	None	LTA	7	20	10	9/7/2011	0.6	1193.1
50	0	None	LTA	7	20	1	9/7/2011	0.7	834.1
50	0	None	LTA	7	20	0.1	9/7/2011	0.9	543.0
50	0	None	LTA	7	45	10	9/13/2011	0.9	331.8
50	0	None	LTA	7	45	1	9/13/2011	1.2	166.1
50	0	None	LTA	7	45	0.1	9/13/2011	1.5	79.3
50	0	None	LTA	7	45	0.01	9/13/2011	2.3	36.4
50	0	None	LTA	7.1	4	10	9/1/2011	0.6	2085.8
50	0	None	LTA	7.1	4	1	9/1/2011	0.6	1708.1
50	0	None	LTA	7.1	4	0.1	9/1/2011	0.7	1345.7
50	0	None	LTA	7.1	20	10	9/7/2011	0.5	1153.8
50	0	None	LTA	7.1	20	1	9/7/2011	0.6	806.3
50	0	None	LTA	7.1	20	0.1	9/7/2011	0.5	520.5
50	0	None	LTA	7.1	45	10	9/13/2011	0.4	321.1
50	0	None	LTA	7.1	45	1	9/13/2011	0.1	160.8

%RAP	%RAS	Additive	Aging	Voids (%)	Temp (Deg C)	Freq (Hz)	Test Date	Phase (deg)	E* (ksi)
50	0	None	LTA	7.1	45	0.1	9/13/2011	0.4	77.2
50	0	None	LTA	7.1	45	0.01	9/13/2011	0.4	36.2
50	0	None	LTA	6.8	4	10	9/1/2011	0.6	2354.0
50	0	None	LTA	6.8	4	1	9/1/2011	0.5	1903.6
50	0	None	LTA	6.8	4	0.1	9/1/2011	0.5	1473.0
50	0	None	LTA	6.8	20	10	9/7/2011	0.4	1304.2
50	0	None	LTA	6.8	20	1	9/7/2011	0.6	893.1
50	0	None	LTA	6.8	20	0.1	9/7/2011	0.6	569.1
50	0	None	LTA	6.8	45	10	9/13/2011	1.2	369.4
50	0	None	LTA	6.8	45	1	9/13/2011	1.3	188.7
50	0	None	LTA	6.8	45	0.1	9/13/2011	1.2	91.8
50	0	None	LTA	6.8	45	0.01	9/13/2011	1	42.7
50	0	Cyclogen	STA	7.2	4	10	9/19/2011	0.5	2064.6
50	0	Cyclogen	STA	7.2	4	1	9/19/2011	0.6	1521.7
50	0	Cyclogen	STA	7.2	4	0.1	9/19/2011	0.5	1048.9
50	0	Cyclogen	STA	7.2	20	10	9/20/2011	0.4	917.1
50	0	Cyclogen	STA	7.2	20	1	9/20/2011	0.2	535.3
50	0	Cyclogen	STA	7.2	20	0.1	9/20/2011	0	286.9
50	0	Cyclogen	STA	7.2	45	10	9/22/2011	0.3	190.4
50	0	Cyclogen	STA	7.2	45	1	9/22/2011	0.7	81.0
50	0	Cyclogen	STA	7.2	45	0.1	9/22/2011	1.5	35.8
50	0	Cyclogen	STA	7.2	45	0.01	9/22/2011	2	18.9
50	0	Cyclogen	STA	7.1	4	10	9/19/2011	0.3	2218.5
50	0	Cyclogen	STA	7.1	4	1	9/19/2011	0.2	1660.7
50	0	Cyclogen	STA	7.1	4	0.1	9/19/2011	0.1	1161.3
50	0	Cyclogen	STA	7.1	20	10	9/20/2011	0.2	977.1
50	0	Cyclogen	STA	7.1	20	1	9/20/2011	0.3	577.0
50	0	Cyclogen	STA	7.1	20	0.1	9/20/2011	0.8	314.2
50	0	Cyclogen	STA	7.1	45	10	9/22/2011	0.8	191.3
50	0	Cyclogen	STA	7.1	45	1	9/22/2011	1.7	82.1
50	0	Cyclogen	STA	7.1	45	0.1	9/22/2011	2.1	37.2
50	0	Cyclogen	STA	7.1	45	0.01	9/22/2011	2	20.0
50	0	Cyclogen	STA	7.2	4	10	9/19/2011	1	2083.8
50	0	Cyclogen	STA	7.2	4	1	9/19/2011	1	1557.9
50	0	Cyclogen	STA	7.2	4	0.1	9/19/2011	0.9	1080.7
50	0	Cyclogen	STA	7.2	20	10	9/20/2011	0.6	901.6
50	0	Cyclogen	STA	7.2	20	1	9/20/2011	0.6	526.3
50	0	Cyclogen	STA	7.2	20	0.1	9/20/2011	0.8	279.3
50	0	Cyclogen	STA	7.2	45	10	9/22/2011	0.5	169.7
50	0	Cyclogen	STA	7.2	45	1	9/22/2011	1.2	71.7

%RAP	%RAS	Additive	Aging	Voids (%)	Temp (Deg C)	Freq (Hz)	Test Date	Phase (deg)	E* (ksi)
50	0	Cyclogen	STA	7.2	45	0.1	9/22/2011	1.6	33.0
50	0	Cyclogen	STA	7.2	45	0.01	9/22/2011	0.8	19.0
50	0	Cyclogen	LTA	7.1	4	10	9/27/2011	0.6	2356.1
50	0	Cyclogen	LTA	7.1	4	1	9/27/2011	0.7	1831.0
50	0	Cyclogen	LTA	7.1	4	0.1	9/27/2011	0.7	1347.0
50	0	Cyclogen	LTA	7.1	20	10	9/28/2011	0.8	1127.8
50	0	Cyclogen	LTA	7.1	20	1	9/28/2011	0.8	706.8
50	0	Cyclogen	LTA	7.1	20	0.1	9/28/2011	0.7	410.6
50	0	Cyclogen	LTA	7.1	45	10	9/29/2011	1.1	266.3
50	0	Cyclogen	LTA	7.1	45	1	9/29/2011	1.4	124.2
50	0	Cyclogen	LTA	7.1	45	0.1	9/29/2011	2	58.5
50	0	Cyclogen	LTA	7.1	45	0.01	9/29/2011	3.1	32.1
50	0	Cyclogen	LTA	7.2	4	10	9/27/2011	0.2	2213.0
50	0	Cyclogen	LTA	7.2	4	1	9/27/2011	0.3	1725.7
50	0	Cyclogen	LTA	7.2	4	0.1	9/27/2011	0.2	1277.2
50	0	Cyclogen	LTA	7.2	20	10	9/28/2011	0.4	1051.2
50	0	Cyclogen	LTA	7.2	20	1	9/28/2011	0.6	657.2
50	0	Cyclogen	LTA	7.2	20	0.1	9/28/2011	0.7	380.4
50	0	Cyclogen	LTA	7.2	45	10	10/5/2011	0.1	251.9
50	0	Cyclogen	LTA	7.2	45	1	10/5/2011	0.2	115.9
50	0	Cyclogen	LTA	7.2	45	0.1	10/5/2011	0.1	52.7
50	0	Cyclogen	LTA	7.2	45	0.01	10/5/2011	1	26.0
50	0	Cyclogen	LTA	7	4	10	9/27/2011	0.4	2345.6
50	0	Cyclogen	LTA	7	4	1	9/27/2011	0.4	1837.3
50	0	Cyclogen	LTA	7	4	0.1	9/27/2011	0.4	1361.8
50	0	Cyclogen	LTA	7	20	10	9/28/2011	0.6	1141.2
50	0	Cyclogen	LTA	7	20	1	9/28/2011	0.8	720.8
50	0	Cyclogen	LTA	7	20	0.1	9/28/2011	0.9	419.4
50	0	Cyclogen	LTA	7	45	10	10/5/2011	0.5	265.0
50	0	Cyclogen	LTA	7	45	1	10/5/2011	0.5	121.0
50	0	Cyclogen	LTA	7	45	0.1	10/5/2011	0.9	54.8
50	0	Cyclogen	LTA	7	45	0.01	10/5/2011	1.3	27.3

APPENDIX F RESULTS OF ENERGY RATIO TEST PROCEDURE

Properties	Virgin	50% RAP	50% RAP + RA	20% RAP + 5% RAS	20% RAP + 5% RAS + RA
%RAP	0	50	50	20	20
%RAS	0	0	0	5	5
Additive	None	None	Cyclogen	None	Cyclogen
m-value	0.380	0.340	0.347	0.334	0.378
D_1	5.19E-07	3.54E-07	3.85E-07	5.02E-07	5.90E-07
S_t (Mpa)	1.960	2.210	2.470	2.420	2.240
M_r (Mpa)	10.777	13.543	12.397	11.557	11.020
Fracture Energy (kJ/m3)	3.5	0.7	1.8	2.2	2.3
$DCSE_{HMA}$ (kJ/m3)	3.3	0.5	1.6	1.9	2.1
Stress (psi)	150	150	150	150	150
a	4.91E-08	4.77E-08	4.63E-08	4.66E-08	4.76E-08
$DSCE_{MIN}$ (kJ/m3)	0.592	0.297	0.354	0.410	0.683
Energy Ratio	5.61	1.75	4.40	4.75	3.03
Rate of Creep Compliance	2.73E-09	1.26E-09	1.46E-09	1.68E-09	3.04E-09

APPENDIX G RESULTS OF IDT TEST PROCEDURE

Temp (degC)	Loading Time (sec)	Creep Compliance (1/GPa)				
		Control	50% RAP	50% RAP + RA	20% RAP + 5% RAS	20% RAP + 5% RAS + RA
-20	1	0.036	0.027	0.043	0.042	0.042
-20	2	0.038	0.028	0.045	0.044	0.044
-20	5	0.041	0.03	0.047	0.046	0.047
-20	10	0.045	0.031	0.05	0.048	0.05
-20	20	0.048	0.033	0.053	0.051	0.053
-20	50	0.057	0.036	0.058	0.056	0.058
-20	100	0.065	0.039	0.062	0.06	0.063
-10	1	0.053	0.052	0.051	0.052	0.06
-10	2	0.058	0.055	0.054	0.056	0.065
-10	5	0.064	0.059	0.06	0.06	0.071
-10	10	0.069	0.063	0.065	0.066	0.076
-10	20	0.076	0.067	0.072	0.071	0.083
-10	50	0.086	0.073	0.084	0.08	0.095
-10	100	0.096	0.078	0.095	0.088	0.105
0	1	0.082	0.073	0.072	0.078	0.079
0	2	0.091	0.079	0.078	0.087	0.087
0	5	0.104	0.089	0.089	0.098	0.1
0	10	0.117	0.099	0.099	0.111	0.111
0	20	0.134	0.109	0.112	0.124	0.127
0	50	0.164	0.129	0.134	0.149	0.151
0	100	0.195	0.144	0.154	0.174	0.177

Indirect Tensile Strength at -10C (Mpa)	Control	50% RAP	50% RAP + RA	20% RAP + 5% RAS	20% RAP + 5% RAS + RA
	4.32	4.09	3.84	3.72	3.39

APPENDIX H RESULTS OF OVERLAY TESTING

Mix ID	Sample Air Voids (%)	Maximum Load (lb)	No. of Cycles to Failure
Virgin	6.2	781.9	4873
Virgin	6	811.7	4524
Virgin	6.3	859.8	3708
50% RAP	6.6	1145.7	114
50% RAP	6.7	1129.7	220
50% RAP	6.4	1183.0	66
50% RAP + RA	7.1	929.5	430
50% RAP + RA	7	933.6	589
50% RAP + RA	7.1	947.6	293
20% RAP + 5% RAS	6.4	954.8	272
20% RAP + 5% RAS	7.8	809.7	575
20% RAP + 5% RAS	7.2	870.5	159
20% RAP + 5% RAS + RA	6.5	950.1	406
20% RAP + 5% RAS + RA	7.4	879.1	224
20% RAP + 5% RAS + RA	6.4	884.1	1514

APPENDIX I RESULTS OF APA TESTING

%RAP	%RAS	Additive	Temp (°C)	Air (%)	Manual Rut (25-Final) (mm)	Automated Rut (mm)
20	5	Cyclogen	64	6.8	3.045	2.810
20	5	Cyclogen	64	6.9	3.505	3.560
20	5	Cyclogen	64	6.8	3.845	3.760
20	5	Cyclogen	64	6.6	3.300	3.010
20	5	Cyclogen	64	6.9	5.670	4.390
20	5	Cyclogen	64	6.7	5.000	4.000
20	5	None	64	7.1	2.290	2.270
20	5	None	64	6.8	2.770	2.510
20	5	None	64	7.5	3.775	2.610
20	5	None	64	7.4	3.140	2.650
20	5	None	64	7.6	3.930	2.900
20	5	None	64	7.0	2.520	2.480
50	0	Cyclogen	64	6.9	3.835	3.690
50	0	Cyclogen	64	7.0	5.360	4.550
50	0	Cyclogen	64	6.9	4.855	4.860
50	0	Cyclogen	64	7.0	4.315	3.270
50	0	Cyclogen	64	6.9	5.525	4.490
50	0	Cyclogen	64	6.9	6.625	4.710
0	0	None	64	7.1	4.390	5.426
0	0	None	64	7.0	2.865	4.957
0	0	None	64	7.0	3.600	7.265
0	0	None	64	7.2	2.075	5.886
0	0	None	64	7.2	0.605	4.246
0	0	None	64	7.3	3.530	6.587
0	0	None	64	7.3	2.670	7.041
50	0	None	64	7.1	1.820	3.186
50	0	None	64	6.9	0.920	2.893
50	0	None	64	6.9	1.580	3.014
50	0	None	64	7.1	1.040	2.471
50	0	None	64	6.9	1.025	2.884
50	0	None	64	6.9	1.220	2.794